Timis, Elisabeta Cristina; Hutchins, Michael George; Cristea, Vasile Mircea. 2022. **Advancing understanding of in-river phosphorus dynamics using an advection-dispersion model (ADModel-P).**

The definitive version was published in *Journal of Hydrology* (2022) 612 (B): 128173. https://doi.org/10.1016/j.jhydrol.2022.128173

Advancing understanding of in-river phosphorus dynamics using an advection-dispersion model (ADModel-P)

Elisabeta Cristina Timis [a*], Michael George Hutchins [b], Vasile Mircea Cristea [a]

[a] *Babes-Bolyai University, Department of Chemical Engineering, Computer Aided Process Engineering Research Centre, No. 11, Arany Janos Street, 400028, Cluj-Napoca, Cluj, Romania*

[b] *UK Centre for Ecology and Hydrology Wallingford, Maclean Building, Crowmarsh Gifford, Wallingford, Oxfordshire, OX10 8BB, UK.*

Abstract

The objectives of the present research are (1) to predict phosphorus compounds transport along river stretches at high spatio-temporal resolution by developing an original approach based on advection-dispersion modelling (ADModel-P); (2) to advance the understanding of in-stream phosphorus transformation processes, and (3) to explore their relation to controlling factors (water temperature, seasonality and water flow). For a case study of the River Swale (UK) modelling results, in agreement with results based on experimental data, show that resuspension is the largest contributor to the variability of organic phosphorus, while adsorption-desorption are the largest contributors to the variability of soluble reactive phosphorus. Additionally, simulations reveal that conversion of inorganic to organic forms is important. In-channel sinks appear more important than sources for Soluble Reactive Phosphorus (SRP) during 80% of the time, while there is no clear evidence that Organic Phosphorus (OP) sinks or sources are dominant except the beginning of spring (around 20% of the total time). The findings are valuable because they advance knowledge regarding: (1) which in-stream processes are important; (2) values associated to transformation rates for mineralization, sedimentation, resuspension, uptake, adsorption - desorption; (3) at which times rivers are net sources or sinks and which source/sink processes might be dominant. ADModel-P is a robust model which has the benefits of simple field data requirements (compared to more complex models) and less assumptions (e.g. compared to simple models assuming perfect mixing in reaches) but without the drawbacks of lack of process representation

* corresponding author: elisabeta.timis@ubbcluj.ro

to enable confidence in predictions to change. There is extensive scope for transferability to other rivers: rate constants can be estimated from easily attainable information on water temperature, seasonality and water flow.

Keywords: phosphorus in-stream transformations; advection dispersion pollutant transport model; mineralization; sedimentation - resuspension; uptake; adsorption - desorption.

1 Introduction

Phosphorus (P) compounds are among the most important freshwater nutrients of critical concern. The increased attention they receive currently at global level is motivated by their key role in the agriculture (e.g. fertilizers) and in the ecosystem dynamics (e.g. as limiting nutrients for algae production). Increased loads of phosphorus to waterbodies is usually the primary driver for the eutrophication of freshwater bodies (Charlton et al., 2018; Colborne et al., 2019; Zinabu et al., 2018). The European Environment Agency's databases on the status and quality of Europe's water resources (Waterbase) shows evidence that the average concentration of phosphates in European rivers is larger during the period 2000–2017 compared to the period 1992–2017, even if a decrease of 1.6 % per year is indicated over the last two-three decades (EEA, 2019), mainly attributed to the improved waste water treatment technologies. Among river water bodies assessed by the Environment Agency in England, 55% were at less than good ecological status with respect to P concentrations in 2016 (Environment Agency, 2018), while an earlier report indicates the figure to be just 45% (Environment Agency, 2012). Concern surrounds persistence of elevated levels due to release of “legacy” P held in riverbed sediments that offset benefits of reduced pollutant load from the land and other sources such as improved waste water treatment. Moreover, recent research shows that P concentrations are and will remain high enough to fail P standards until 2050 (Charlton et al., 2018; Jarvie et al., 2018; Hutchins et al., 2016; Ockenden et al., 2016) or are greater than ecologically limiting thresholds (Riley et al., 2018) and emphasise the increasing risk of eutrophication. Dangers, associated principally to P compounds, are long-established and widely investigated for rivers in England and worldwide (Harrison et al., 2019a and 2019b; Charlton

et al., 2018; Zelenakova et al., 2018; Enea et al., 2017; Ji, 2017; Hutchins et al., 2016; Koraqi et al., 2016; Romanescu et al., 2016; Iordache and Dunea, 2013).

In this context, appropriate countermeasures to water quality degradation, with respect to P, should be underpinned by deep understanding of the behaviour and fate of P species and on the prediction of its future trends. Recent work underlines the important role of water quality models which include P concentrations (Riley et al., 2018; Tuo et al., 2015; Charlton et al., 2018), to support high quality decision making and water management. The mathematical modelling of water quality facilitates both understanding of phenomena and its prediction, even in cases where the availability of experimental data is limited (Ani et al., 2009). Such modelling can be carried out at different levels of magnitude and detail, starting from the small scale (hundreds of meters of river stretch) to the global scale (see the models discussed by Harrison et al., 2019b), depending on the area of interest, its particularities and the needs. With respect to the resolution in terms of space and time, the spectrum of approaches extends between: (A) catchment scale modelling (describing a catchment or multiple catchments, not necessarily high-resolution in terms of space and time), mainly based on usual long-term monitoring data (Keraga et al., 2019; Srinivas and Singh, 2018); and (B) modelling of river stretches based on high resolution data (multiple monitoring points along the stretch, where measurements of channel characteristics, hydrodynamic data and water quality data are needed), such as ADModel for nitrogen (Ani et al., 2011).

In terms of advancing system understanding, river P transport studies of both types have proven valuable in many respects: (a) facilitate understanding of catchment scale processes and patterns (Lupi et al., 2019; Wade et al., 2002) including use of storm-event data (Ramos et al., 2015); (b) understand nutrient (including P) interactions between water and sediment phases (Wijesiri et al., 2019; Yuan et al., 2019; Tye et al., 2016) or the contribution of streambanks to in river P load (Fox et al., 2016); (c) assess catchment scale ecological quality status (Charlton et al., 2018); (d) make correlations between in-river compounds (Wade et al., 2002; Neal et al., 2010); (e) explore relations between chemical species concentration (including P) and different influences, such as water flow, seasonality, temperature, certain types of sources (Charlton et al., 2018; Ockenden et al., 2016; Cooper et al., 2015; Wade et al., 2002);

and (f) identification and/or understanding of P pollution sources (alone or along with other nutrients), (Colborne et al., 2019; Liberoff et al., 2019; Records et al., 2016; Ramos et al., 2015).

During recent years river stretch studies (type B) including high resolution measurements of P species and advective–dispersive non-conservative transport have become less common. This is most probably due to the difficulties and great costs associated to gathering the needed high resolution data (which despite recent advances (Halliday et al., 2015; Rode et al., 2016) is still not commonplace), and also a change in focus towards studies covering larger spatial scales. Valuable recent studies include those of Dou et al. (2018) and Nguyen et al. (2018), while earlier studies are a lot more abundant, as shown by Mateus et al. (2018), Gao and Li (2014), Wang et al. (2013), Tsakiris and Alexakis (2012) or Ani et al. (2010).

For effective basin-scale management it is important to maintain small-scale modelling development to inform appropriate and sufficiently accurate process representation in larger-scale models (Tang et al., 2019). The extent to which in-channel transformations are important in determining catchment scale fluxes is unclear. Conservative or black box modelling approaches with simple dependencies on residence time (Zhang et al., 2017) or sedimentation (Jackson-Blake et al., 2017) may provide sufficient representation, but this merits further attention. In this context, ADModel, a model based upon detailed representation of pollutant advection and dispersion has been successfully developed for simulation of nitrogen compounds (Ani et al., 2011), and performs comparably to a contrasting but extensively tested model (QUESTOR: Boorman 2003a, 2003b) that assumes complete mixing in asset of reaches. The advection-dispersion approach was calibrated and evaluated by considering the transport parameters (e.g. dispersion coefficients, convective velocity) and associated nutrient nitrogen transformations: nitrate and ammonium. Given the need to better understand phosphorus dynamics in rivers it is important to build on the approach by developing from first principles a compatible approach for phosphorus. The potential that would then arise for an integrated approach covering multiple nutrient determinands is of much value.

The River Swale in north-east England has been the focus or a part of a wide range of studies on phosphorus: (i) speciation in the main channel based on weekly river monitoring data (Jarvie et al., 1998) including the influence of various types of wastewater (Neal et al., 2010); (ii) influence of point and diffuse inputs on the River Swale and its major tributaries (House and Warwick, 1998a); (iii) modelling of point and diffuse sources in three river catchments, using load appointment and export coefficient approaches, focusing on Total Phosphorus, TP (Bowes et al., 2008); (iv) estimation of mass balances, seasonally-variable losses and gains of nutrients along reaches under differing flow conditions including stable low flows and overbank floods (House and Warwick, 1998b; Bowes and House, 2001; Bowes et al., 2003; Bowes et al., 2008). These lines of evidence have supported the existence of groundwater inputs of varying importance depending on discharge levels; (v) phosphorus–discharge hysteresis during storm events (Bowes et al., 2005; House and Warwick, 1998a); (vi) sediment transport and interactions (Kim et al., 2006; Smith et al., 2003; Owens and Walling, 2003; House and Warwick, 1999; House et al., 1998).

Despite a breadth of process-based understanding in the Swale, a detailed modelling approach, as adopted in ADModel-P, is lacking. Findings from process-based studies will be revisited later to provide invaluable context for a modelling study on the P transformations.

Therefore the objectives of the present paper are (1) to offer a new validated detailed modelling tool (ADModel-P) for the prediction of P compounds transport along a stretch of River Swale at sub-daily resolution, based on principles of advection and dispersion previously applied for nitrogen simulation; (2) to advance the understanding and significance of in-stream P transformation processes, (3) to explore their relation to controlling factors, namely water temperature, seasonality and water flow, and (4) offer a P compounds transformations model (using field data easy to collect) transferable to other case studies.

In terms of river pollutant transport the present research contributes to:

i. the detailed representation of phenomena which empowers good prediction efficiency of concentrations (and in the same time does not make it a too complex model);

ii. the use of easily attainable field data (water flow, water temperature and seasonality) to generate empirical relations to express the dynamics of process rates. This is in contrast to existing mechanistic models which require detailed characterisations and extensive assumptions of channel properties potentially making applications complex and challenging;

iii. the original perspective of approaching correlations between phosphorus compounds transformation rates and resulting in-stream concentrations on one side and their main controlling factors (sources of P, water flow, water temperature and seasonality) on the other side.

Section 2 of the paper describes the study area and field data. Section 3 describes the model background and the development process. Section 4 describes the transformations model development (the context of P compounds transformations and their representation in existing models) and describes the model in detail. Section 5 comprises results and discussions, starting with results of the new developed transformations model discussed in conjunction to previous findings (sub-section 5.1). In the next sub-section (5.2) the results of ADModel-P for concentration prediction are presented and analysed. The original perspective of approaching correlations between controlling factors, P transformations and concentrations follows (sub-section 5.3), while sub-section 5.4 places the findings in the context of other river P models.

2 Study area and field data

The investigated area of River Swale (further referred to also as the river stretch or the study area) is 54km long, delimited at the upstream end by Catterick (National Grid Reference, NGR, SE225994508) and at the downstream end by Crakehill (NGR SE426734). It includes three major tributaries (River Wiske, Bedale Beck and Cod Beck) and 15 minor tributaries. This River Swale Catchment is a part of the greater River Ouse Catchment, presented in Fig. 1.

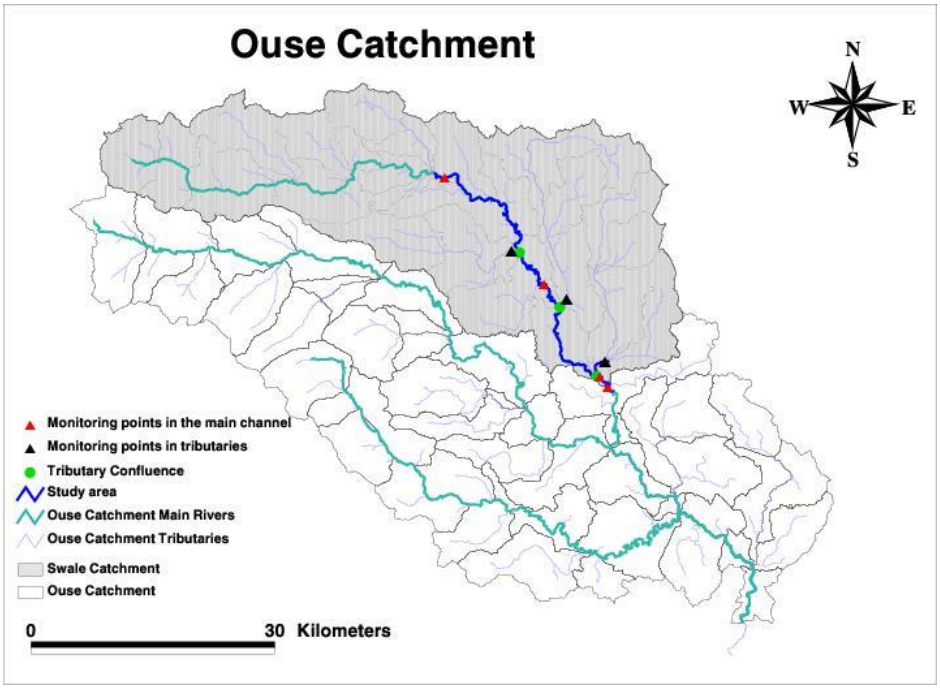

Fig. 1. The map of the study area and the Swale Catchment in the greater Ouse Catchment.

The monitoring data used by House and Warwick (1998a and 1998b) and Bowes and House (2001) along with additional field data will be used. The focus is on data from the late 1990s, which provides a valuable perspective on model development as it covers a period where in general in-river legacy stores had not yet started to be depleted. This is likely still the case in sensitive environments where large point sources (as targeted by EU Urban Wastewater Treatment Directive legislation) are absent.

The field data include measurements at the monitoring stations (for the channel width, water depth, water flow rate and P species concentrations) and estimations based on GIS (for the river bed slope) corresponding to the main stream of the River Swale and the three major tributaries. The ten intensive monitoring campaigns carried out at temporal resolution up to 3 hours are briefly described in Table 1.

Campaign number	Campaign timing	Total duration [h]	Water flow range [m^3/s]	SRP range [mg/L]	OP range [mg/L]	Water temperature range [°C]	Seasonality factor range
C1.	September 1994	43	0.80 - 47.80	0.01 - 1.71	0.01 - 0.33	8.4 - 12.4	0.048 - 0.049
C2.	February 1995	40	0.80 - 41.50	0.01 - 0.47	0.03 - 0.56	4.0 - 7.1	0.377 - 0.381
C3.	October 1995	107	0.17 - 5.12	0.03 - 3.24	0.00 - 2.21	6.0 - 10.0	0.009 - 0.011
C4.	February 1996	117	2.66 - 57.70	0.01 - 0.38	0.00 - 0.50	0.7 - 4.7	0.349 - 0.371
C5.	April 1996	108	0.43 - 16.60	0.02 - 1.42	0.00 - 1.01	7.0 - 11.0	0.830 - 0.857
C6.	March 1998	190	0.53 - 196.67	0.01 - 0.97	0.00 - 6.34	5.0 - 9.0	0.414 - 0.464
C7.	July 1998	190	0.30 - 53.31	0.02 - 1.72	0.00 - 2.93	15.0 - 19.0	0.463 - 0.582
C8.	October 1998	190	0.22 - 29.67	0.02 - 2.37	0.00 - 0.82	10.2 - 14.0	0.019 - 0.026
C9.	July 1999	264	0.57 - 30.65	0.02 - 1.15	0.00 - 0.53	15.0 - 19.0	0.445 - 0.610
C10.	February 2000	336	0.55 - 90.39	0.02 - 1.09	0.00 - 1.02	2.9 - 7.0	0.287 - 0.368

Table 1 Description of field data employed for ADModel-P (SRP, Soluble Reactive Phosphorus; OP, Organic Phosphorus). Ranges regard values measured in the main channel and in the three major tributaries. The significance of the seasonality factor is explained in section 4.2.

Different environmental conditions are reflected, as data has been collected during a wide range of events from low discharge (e.g. event C3 in October 1995) to very high discharge during storms (e.g. event C6 in March 1998). The water flow graphs for campaigns C1 to C10 are available in Fig. D. 1 and Fig. D. 2. During these events the concentration of P components in the River Swale is heavily influenced by sinks and sources, which can be represented under two labels (1) in river processes (denominated also transformations), which cause consumption or generation of a certain chemical species and (2) discharges of effluents from outside the river (denominated also pollution sources), which introduce significant amounts of phosphorous presented under different forms (Neal et al., 2010; Withers and Jarvie, 2008). For River Swale there are point and non-point (diffuse) phosphorous sources (Bowes et al., 2008). Point sources (mainly Sewage Treatment Works, STWs) provide a continuous load of phosphorus to the river and strongly influence SRP, mainly during low flow. Their influence is less significant during high flows due to dilution. Non-point sources (agricultural and farming activities) predominate mainly during high flows (confirmed also by House and Warwick, 1998a), being associated with runoff and soil erosion and are the dominant sources of soluble unreactive phosphorus (SUP) (increasing TDP and consequently TP) and particulate phosphorus (PP) (increasing TP). Pollution sources are included in ADModel-P, as inputs, but their detailed investigation is out of the scope of the present paper. In contrast, in-river P transformations are comprehensively discussed.

The concentrations field data (measurements of phosphorus species concentrations) at the River Swale monitoring stations has been made public on HydroShare (Hutchins and Timis, 2020). This data

is part of a larger freely available accredited dataset by Leach et al. (2013), including nutrient concentrations also for the River Swale. The water flow data is available online in the UK National River Flow Archive (link available in the references list) at the specific locations for the two sites: the upstream end of the investigated river stretch (station number 27090) and at the downstream end of the river stretch (station number 27071).

3 Methodology

3.1 Model background

ADModel-P is based on the one-dimensional (1D) advection-dispersion equation (ADE) for mass transport along distributed parameters systems (such as the rivers).

$$\frac{\partial c}{\partial t} = \frac{\partial}{\partial x}\left(D\frac{\partial c}{\partial x}\right) - \frac{\partial (cV)}{\partial x} + S \pm T$$

The equation describes the evolution in time (t [s]) of the concentration (c [mg/L]) of a chemical species along the river reach (x [m]), while the pollutant is discharged from sources (S [mg/s L]) and it is consumed or produced in the river trough processes expressed by the rate of transformation (T [mg/s L]). The concentration dynamics is also affected by the convective transport velocity (V [m/s]) and the longitudinal dispersion coefficient (D [m^2/s]).

For the development of ADModel-P an analytical solution of the 1D ADE suitable to describe the pollutant dynamics during the continuous point discharge (Pujol and Sanchez-Cabeza, 2000) has been implemented in MATLAB together with a model for the transformations. The appropriate description of transformation processed during the in-stream transport is the main challenge related to the ADE based approach.

3.2 The steps to calibrate and verify the model

The dynamic representation of transformation rates in ADModel-P has been guided by identifying semi-empirical models to estimate the rates for each transformation process. A stepwise process was implemented (Fig. 2).

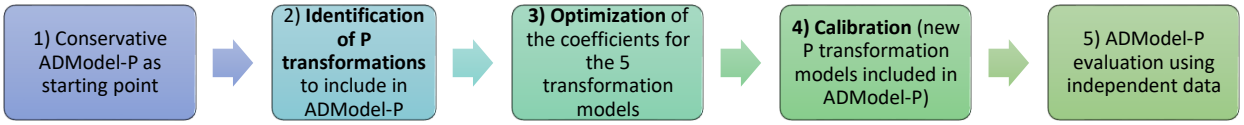

Fig. 2. Steps for ADModel-P calibration and evaluation for P compounds

1) The start point was a conservative advection-dispersion model with no transformations.

2) Representing the phosphorous transformations, which involves two sub-steps identifying (i) which transformations to include and (ii) suitable mathematical relationships (initial form, to be refined later during preliminary calibration) to represent their controlling factors. A robust pollutant transport model needs identification of optimal complexity, as explored by Jackson-Blake et al. (2017) who sought opportunity to simplify the complex INCA-P model. For ADModel-P the identified transformations model (see section 4) involves 5 processes each expressed mathematically with empirical rate coefficients for calibration.

3) Optimisation of the empirical rate coefficients (the eight M and R described in Table 3). The MATLAB built-in optimization function, *fmincon*, has been employed as basis for the optimization framework developed for ADModel-P. The framework key components are: (1) the objective function which calculates the difference between the two types of concentration vectors (estimated vs. measurements for both SRP and OP) based on the widely-used Nash Sutcliffe model efficiency coefficient (NSE) (Nash and Sutcliffe, 1970); (2) the non-linear constraints function with respect to the SRP and OP concentrations, in order not to allow negative values of the estimated concentrations; (3) lower and upper limits for the decision variables (M and R coefficients) and (4) the starting point for each decision variable. It is crucial how the options of the optimization function (*optimoptions*) are defined, because different kind of settings related to issues such as the optimization algorithm, the tolerances or the search stopping criteria could lead to very different solutions. The eight decision variables are modified automatically by the optimization algorithm at each computation cycle to achieve a minimum value of the objective function (corresponding to the maximum of the NSE coefficient) while

meeting the non-linear constraints, the tolerances and the limits for the decision variables. The initial values of the rate coefficients employed by ADModel-P as start point for the optimization have been estimated based on QUESTOR rates for mineralization and sedimentation (transformations included in QUESTOR, as employed by Hutchins et al. (2010)), while for the other transformations the initial rate coefficients are zero. Observed data for P compounds are taken from 8 of the 10 calibration data sets excluding two campaigns to be used later for model evaluation.

4) The optimum forms of the models for transformations have been further introduced in ADModel-P in order to finalize its calibration. Following implementation in ADModel-P, applications demonstrate model performance against experimental data for the eight model development campaigns.

5) ADModel-P was later verified using independent data from the remaining two monitoring campaigns.

Multiple runs of preliminary model calibration followed by evaluation (steps 3 to 5) have been carried out employing each time two different independent campaigns for the model evaluation. The selection of the two evaluation campaigns has been done fulfilling two main rules: (1) evaluation events should take place in different times of the year, in order to ensure variability over seasonality; and (2) evaluation events should take place at different flow regime. Otherwise, the combinations are random. The purpose of these preliminary runs was to identify the trends of transformation processes in relation to controlling factors, in order to validate the most suitable form of the equations for the process rates (initially identified in step 2 above and in final form as described in section 4.2) and the appropriate settings for the optimization framework (step 3 above). The results in terms of goodness of fit associated to the preliminary runs are presented in Table B. 1 (in Appendix B). Further, the finalised identification of equations and optimization settings has been implemented in ADModel, which then underwent a final round of calibration and evaluation employing a chosen data splitting option (#2 in Table B. 1 in Appendix B).

ADModel-P has been made public on HydroShare (Timis, 2021).

4 The identification of the phosphorus transformations model to employ

4.1 Phosphorus components and transformations

Phosphorus is present in multiple constituents of the river ecosystem (algae, zooplankton and aquatic animals; water; river channel, e.g. sediments, river banks soil) and under multiple forms (Ji, 2017; Chau, 2005; Loucks and van Beek, 2017). Terminology has not always been consistent with different appellations or assumptions used and wider terms often introduced (e.g. organic P and particulate P used as interchangeable), hence these are comprehensively related in tabular (Table A. 1 in Appendix A) and graphical (Fig. 3) as employed in the literature (Charlton et al., 2018; Dou et al., 2018; Ji, 2017; Tye et al., 2016; Tuo et al., 2015; Neal et al., 2010; Bowes et al., 2005 and 2003; House, 2003; Wade et al., 2002; House and Warwick, 1998a; Bowie et al., 1985).

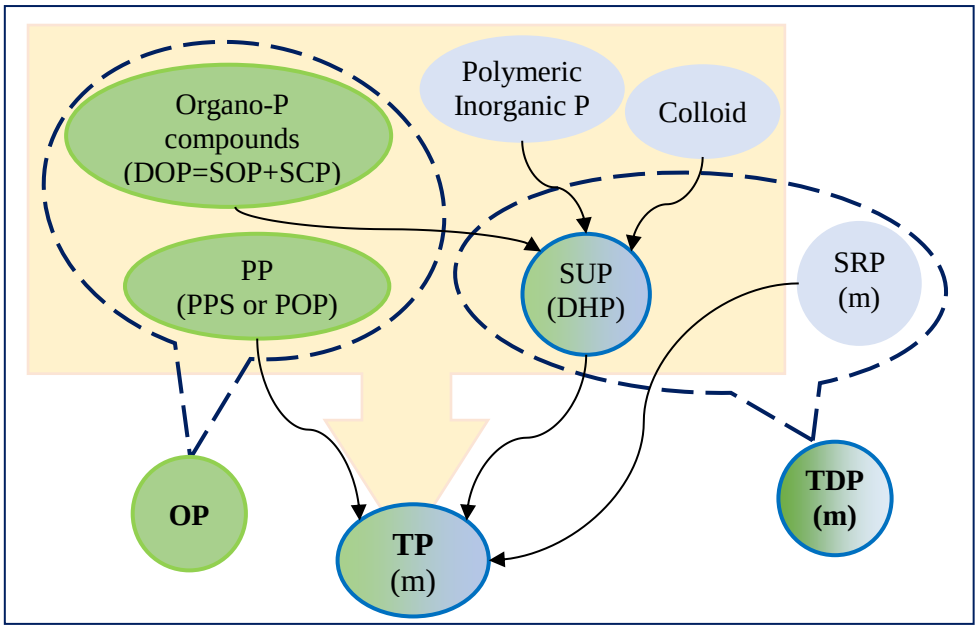

Fig. 3. In-stream phosphorus compounds and their general relations, not involving processes. Acronyms and explanations are available in Table A. 1 in Appendix A (m = measurable, P, Phosphorus; DOP, Dissolved Organic P; SOP, Soluble Organic P; SCP, Soluble Complex P; PPS, POP or PP, Particulate P; OP, Organic P; TP, Total P; SUP or DHP, Soluble Unreactive P; SRP, Soluble Reactive P; TDP, Total Dissolved P).

Visual representation of processes (associated to models and not only) typically uses one of three different approaches, depending on the purpose of the case study: (1) a "generalist" approach employing an all-inclusive P term contained in phases (e.g. P in water and P in sediments, as in Wijesiri et al., 2019); (2) simple representations of the phosphorus cycle, usually involving one type of organic P (under different designations, e.g. OP, PP) and one type of inorganic P (under different designations, e.g. SRP,

IP), (Hutchins et al., 2010, a QUESTOR application including the Swale, and also Srinivas and Singh, 2018; Jackson-Blake et al., 2017; Cooper et al., 2015; Lindenschmidt et al., 2007); and (3) more complex representations, involving more components and multiple interdependencies (Dou et al., 2018; Alam and Dutta, 2016; Kim et al., 2006; Loucks and van Beek, 2017; Bowie, 1985). Robson (2014) states that "catchment - river models are almost universally on the simpler side with respect to their treatment of in-stream processes", sometimes only considering TP and either representing sedimentation alone, or not representing in-stream processes thereby assuming that nutrient sources from outside the river are determinant on the in-river nutrient load. Of the post-2003 river models reviewed by Robson (2014), 74% include less than 3 biogeochemical or ecological processes; and Robson (2014) also states that ecological models for rivers often do not consider phosphorus at all.

There are however a wealth of models taking into account more than one phosphorus species and multiple in-stream processes. The processes either act as sinks or sources for each category of compounds (Table 2). A sub-set of the processes in Table 2 are chosen later for specific modelling of P compounds transport by ADModel-P in River Swale.

Dissolved organic P	**Dissolved inorganic P**
+ excretion by living organisms + respiration of living organisms + plant decay + decomposition of detritus + chemical transformations + release from sediments - chemical processes: mineralization, hydrolysis - sedimentation	+ excretion by living organisms + chemical processes: mineralization of OP, hydrolysis of DOP, oxidation of PP + decomposition of detritus + release from sediments - uptake by plants - sorption by sediments - chemical processes
Particulate organic P	**Sediment P**
+ excretion by living organisms + plankton mortality + zooplankton grazing + decomposition + resuspension - sedimentation - chemical processes: acid oxidation	+ detritus settling + algal settling + sedimentation of PP - sediment decomposition and release - resuspension - chemical processes: mineralization

Table 2 Main transformations governing different types of P forms (P, Phosphorus; OP, Organic Phosphorus; DOP, Dissolved Organic Phosphorus; PP, Particulate Phosphorus): (+) is associated to formation/ sources, while (-) to consumption / sinks

4.2 Phosphorus transformations included in ADModel-P

As stated earlier, P transformation are important in the Swale. House and Warwick (1998b) identified large losses of SRP associated with uptake by the river bed, suspended sediments, macrophytes and algae. Mass balance calculations for TDP, SRP and TP (House 2003) determined the relative importance of riverine processes in controlling P concentrations, and discriminated those in terms of whether they were chemically or physically driven. Bowes et al. (2003; 2005) conclude that the interaction with the river bed and sediments (e.g. mineralisation) is likely significant within the River Swale and that sedimentation and resuspension should be considered by models.

Five categories of in stream P transformations were identified as being important: mineralization, uptake, adsorption-desorption, sedimentation, and resuspension. These are deemed responsible for the loss and/or accumulation of SRP and OP during the transport. The rates of the chemical processes are considered as having first order kinetics, while the physical processes are zero order kinetics. They are mainly influenced by the water temperature (T), water flow (Q) and seasonality. Each rate depends on a particular transformation rate constant (k) as shown in Table 3, where the form of the ADModel-P transformations model equations is presented.

Process	Details
Mineralization	$r_{min} = k_{min}\ c_{OP}$, where $k_{min} = M_{min}\log(1 + T)$ Sink of OP, source of SRP, accounting for the conversion of organophosphates and inorganic polyphosphates to SRP.
Sedimentation	$r_{sed} = k_{sed}\ c_{OP}$, where $k_{sed} = \frac{M_{sed}}{(1+Q)}$ Sink of OP, including the sorption to sediments, sedimentation of PP.
Resuspension	$r_{res} = k_{res}$, where $k_{res} = M_{res}\log(1 + Q) + R_{res}(1 + S)$ Source of OP, including the resuspension of fine sediment, mobilisation of material from the river-bed, in-wash from the floodplain, desorption of P from sediments, resuspension of detritus from the bed sediment followed by the formation of TDP trough the decomposition of plants and detritus. The respiration as a source is included here as well.
Uptake	$r_{upt} = k_{upt}$, where $k_{upt} = M_{upt}\log\left(1 + \frac{1}{1+Q}\right) + R_{upt}\log(1 + S)$ Sink of SRP, accounting for the biological uptake by macrophytes, phytoplankton and benthic algae.
Adsorption - Desorption	$r_{ads-des} = k_{ads-des}\ c_{SRP}$, where $k_{ads-des} = M_{ads-des}\left(1.5 + \log\left(\frac{1}{1+T}\right)\right) + R_{ads-des}$ Sink of SRP, including the sorption of SRP to sediments and to the soil and also the precipitation reactions of SRP. Source of SRP including SRP release from sediments. The resulting value shows the net adsorption as difference between adsorption and desorption.
Where r is the transformation process rate [mg/L s]; T is the measured water temperature [^{o}C]; Q is the water flow [m^3/s]; S is the seasonality factor; c_{SRP} and c_{OP} [mg/L] are the estimated values of concentrations of SRP and OP; k are the transformation rate constants for the processes of uptake k_{upt} [mg/L day], adsorption - desorption $k_{ads-des}$ [1/day], mineralization k_{min} [1/day], sedimentation k_{sed} [1/day], and resuspension k_{res} [mg/L day]; M and R are constants assigned with specific values for each transformation during the model calibration.	

Table 3 Details on the transformations model developed for ADModel-P (OP, Organic Phosphorus; SRP, Soluble Reactive Phosphorus).

The processes included in the SRP uptake by macrophytes, phytoplankton and benthic algae and also those under the formation of TDP through the decomposition of plants and detritus are likely to vary substantially on a seasonal basis. Across the seasons, the aggregated impacts of growth and then decay of primary producers reflect an integration of climate-driven factors on a longer timescale than specific diurnal environmental fluctuations. Therefore, in addition to applying water temperature controls on these transformation rates we invoke seasonal variability into the rate parameters defining sources and sinks. We consider two key variables (the Julian Day number (JDN) and the factor of seasonality or seasonality factor (S)), quantified in the context of the monitoring campaigns (Fig. 4). The JDN allows the representation of multiple events in the time succession they happen and facilitates the

implementation of continuous functions to describe the cyclical influence of seasonality along the monitoring campaigns. A non-dimensional scalar determined by a function based on the sine of the JDN defines S (see Fig. 3), which takes values between 0 (beginning of winter) and 1 (beginning of summer) (with an example provided for 1997). This cyclical variation of S represents the continuous periodicity in the intensity of processes fluctuating cyclically during the year. For example, in the models for resuspension and uptake the intra-annual variability is expected to be strongly determined by S, process rates being expected to increase during spring (Angert et al., 2011). The conjunctive use of JDN and S results in a continuous function describing seasonality in transformation rates models. S is included separately for each transformation rate constant as it may have differing significance.

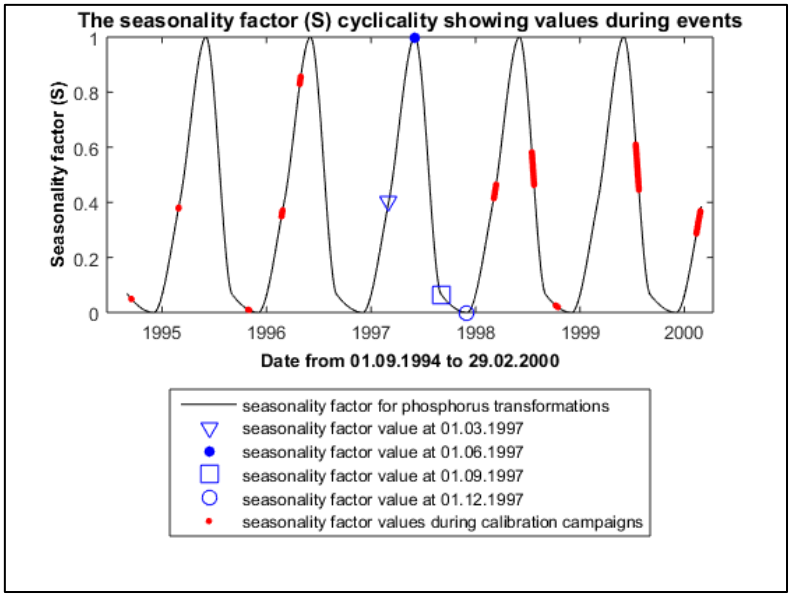

Fig. 4. Representation of the seasonality factor continuity and the values assigned to the monitoring campaigns. x-axis labels correspond to the 1st Jan for each year.

5 Results and discussions

5.1 Transformations model

Values are shown for the M and R coefficients identified during optimization for the calculation of each transformation rate (as in equations in Table 3) and the resulting values of rate coefficients (Table 4). Resuspension is the largest contributor to the variability of OP, while adsorption – desorption are the largest contributors to the variability of SRP (in Table 4 positive values mean net sink).

Transformation	M	R	Process indicators	Calibration			Evaluation		
				Min	Aver	Max	Min	Ave	Max
Mineralization	1.137	NA	k, day $^{-1}$	0.60	2.47	3.41	1.83	3.21	3.41
			rate, g m^{-3} day $^{-1}$	0.03	0.37	2.39	0.11	0.16	0.38
			flux at M4, kg day $^{-1}$	802.95			224.28		
Sedimentation	49.415	NA	k, day $^{-1}$	0.25	4.06	14.00	1.16	4.36	7.62
			rate, g m^{-3} day $^{-1}$	0.02	0.57	1.89	0.07	0.25	0.34
			flux at M4, kg day $^{-1}$	551.16			304.32		
Resuspension	0.315	-0.204	k, g m^{-1} day $^{-1}$	0.19	0.60	1.37	0.28	0.48	0.90
			rate, g m^{-3} day $^{-1}$	0.19	0.54	1.37	0.28	0.42	0.90
			flux at M4, kg day $^{-1}$	1120.25			590.72		
Uptake	0.757	0.382	k, g m^{-3} day $^{-1}$	0.03	0.17	0.34	0.14	0.22	0.28
			rate, g m^{-3} day $^{-1}$	0.03	0.18	0.34	0.14	0.24	0.28
			flux at M4, kg day $^{-1}$	225.17			281.50		
Adsorption – Desorption	3.795	19.064	k, day $^{-1}$	13.39	16.51	22.74	13.39	14.04	18.65
			rate, g m^{-3} day $^{-1}$	0.00	2.11	3.80	0.39	1.76	3.14
			flux at M4, kg day $^{-1}$	2815.09			2077.20		

NA - not applicable; M and R are transformations model coefficients; k – rate coefficients; Max (maximum), Min (minimum), Ave (mean) values are calculated based on the instantaneous values from dynamic series corresponding to each transformation process during calibration and evaluation).

Table 4 Transformation model results obtained during optimization.

Rate coefficients vary during the events (as illustrated in Fig. C.1 in Appendix C) and their variation is influenced by the change of controlling factors, as illustrated in Appendix C: Fig. C.2 for the water flow, Fig. C.3 for the water temperature and Fig. C.4 for the seasonality. Figures show relations to be expected from the basics of the transformations model in Table 3 and reveal agreement with previous findings. Resuspension, followed by mineralization influence the most organic species, while for inorganic species adsorption-desorption processes predominate, as found by House (2003). Highest adsorption rates occur at lowest temperatures (campaign #4: average of 2.7 ^{o}C), whilst lowest rates (i.e. highest desorption) occur during campaign # 7 (average of 17 ^{o}C), findings in agreement with the knowledge that higher water temperatures facilitate anoxic conditions which enhance the release of P from sediments (Han et al., 2022; Mbabazi et al., 2019; House, 2003). There is a positive relationship between water temperature and mineralization rate (as also found by Yuan et al., 2019). Its variability within campaigns is caused by diurnal variation of water temperature (Caissie et al., 2013). Resuspension (which is the largest contributor to the variability of OP) shows greatest relative variability at low flows, as observed by Yuan et al. (2019) and House (2003). Highest rates of resuspension are associated with higher flow and moderate S (seasonality: i.e. early spring). Uptake has the lowest values (Table 4, varying substantially with seasonality showing highest rates in summer when flows are also low. SRP

losses due to uptake are much lower than those due to other sinks, as also found by House (2003) and Jarvie et al. (2005) in nutrient-rich rivers.

5.2 ADModel-P calibration and evaluation results

The ADModel-P inputs consist of the dynamic profiles of water flow and SRP and OP concentrations (1) at the upstream end (acting as boundary condition), (2) at the tributaries and (3) at the actual pollution sources along the stretch. The outputs consist of the dynamic profiles of concentrations of SRP and OP at the downstream end (labelled M4).

Outputs for all 8 development and calibration campaigns and the 2 evaluation campaigns (#2 and #9, kept independent during all earlier stages) are presented (Fig. 5a-d, Fig. E. 1 and Fig. E. 2). It has been decided to simulate all campaigns together as a continuous event (Fig. 5a-d), using concatenated data from individual campaigns (C1 to C5 in Fig. E. 1 and C6 to C10 in Fig. E. 2) in order to test the capability of ADModel to cater for very rapid changes in time at campaign boundaries, as controlling factors and other variables change between campaigns.

It is demonstrated that evaluation campaigns encompass a representative range of conditions with respect to: (1) water flow, storm during campaign #2 and normal flow during campaign #9; (2) water temperature, mean of 6 ^{o}C and 17 ^{o}C for campaigns #2 and #9 respectively; and (3) seasonality, late winter during campaign #2 and mid-summer during campaign #9. Results show that simulations follow the general trend of measurements for both SRP and OP, despite underestimation of peaks in case of events #3, #5 and #7 for the calibration of SRP, events #6 and #8 for the calibration of OP and event #2 for the evaluation of OP. On the other hand, the lowest concentrations of OP are slightly overestimated while the lowest concentrations of SRP are overestimated on few occasions.

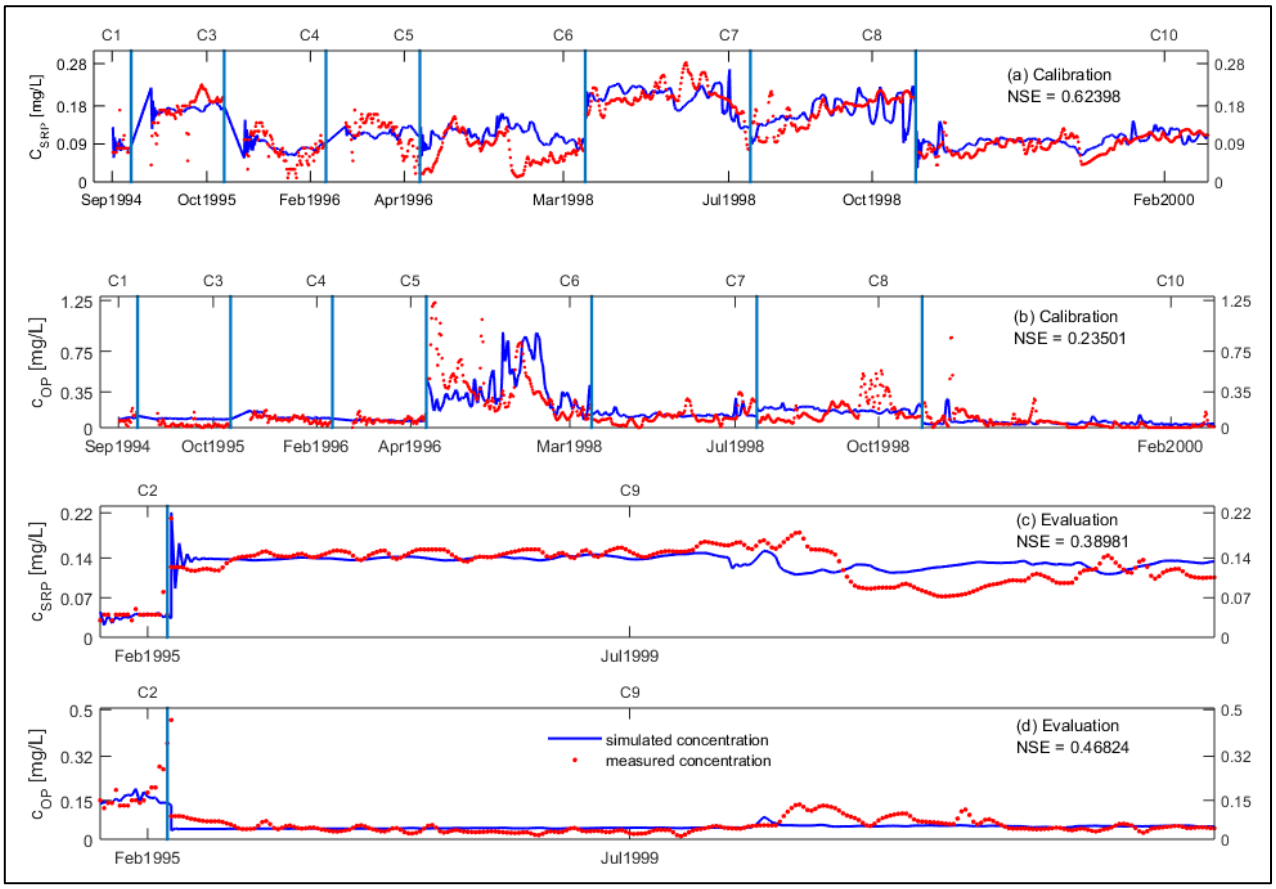

Fig. 5. Dynamic profiles of concentration during calibration (subplots a and b) and evaluation (subplots c and d) presented at hourly resolution at the downstream end of the river stretch. The time x-axes are not continuous. Data from the individual campaigns C1 to C10 carried out during the specified months (Table 1) has been concatenated during simulations. The vertical lines mark the boundaries between C1 to C10.

The ADModel-P performance has been evaluated using the multiple criteria, as shown in Table 5, where values for the non-conservative runs (employing the transformations model) are included. The criteria equations are available in Table B. 2. Additionally, the conservative runs have been assessed with the NSE, and values are -1.65 for the calibration of SRP, -4.77 for the evaluation of SRP, respectively 0.13 and 0.35 for OP. In all occasions, as expected, due to the high importance of transformations, the non-conservative version of the model behaves better compared to the conservative version.

Measured concentration	Unit of measure		Calibration		Evaluation	
			SRP	OP	SRP	OP
Minimum	mg/L		0.01	0.00	0.03	0.04
Average	mg/L		0.32	0.38	0.38	0.16
Maximum	mg/L		0.87	3.76	0.57	0.46
Standard deviation	mg/L		0.05	0.17	0.03	0.05
Model evaluation criteria	**Range**	**Optimal value**	**Calibration**		**Evaluation**	
			SRP	OP	SRP	OP
Nash Sutcliffe efficiency (NSE)	-∞ to 1	1	0.62	0.24	0.39	0.47
Percent bias (PBIAS)	-∞ to ∞	0	-6.78	-6.92	-0.99	11.24
Root mean square error ratio to observations standard deviation (RSR)	0 to ∞	0	0.61	0.87	0.78	0.73
Kling-Gupta Efficiency (KGE)	-∞ to 1	1	0.71	0.53	0.57	0.47
Modified coefficient of determination (bR^2)	0 to 1	1	0.61	0.31	0.43	0.44

Table 5 The range of measured concentrations and the goodness of fit associated to ADModel-P runs at hourly resolution during calibration and evaluation.

Moriasi et al. (2007) discuss models for the streamflow and transport of sediments, nitrogen and phosphorus at larger time steps (mostly daily and monthly) in relation to NSE (range from -∞ to 1), RSR (range from 0 to large positive values) and PBIAS and find that the ‘‘minimally acceptable’’ model performance is indicated by NSE > 0.00, while satisfactory simulations are indicated by NSE > 0.50 together with RSR ≤ 0.70 and PBIAS < ±70% (for nitrogen and phosphorus). The results for detailed hourly simulations of ADModel-P achieve NSE values close to the tresholds of 0.50 (NSE) and respectively 0.70 (RSR) for the calibration of SRP and the evaluation of OP, while for the evaluation of SRP and calibration of OP the values are in the acceptable limits for the model performance. The low values of PBIAS in Table 5 indicate good simulations (according to Gupta et al., 1999 and Moriasi et al., 2007), with small overestimation bias for SRP during calibration and evaluation (the negative values of PBIAS) and for OP during calibration, while there is underestimation bias for OP during evaluation (the positive value of PBIAS). The KGE values between 0.47 and 0.71 indicate good results of ADModel, if taking into account the limit of KGE > 0.3 or NSE > 0.5 mentioned by Knoben et al. (2019) in relation to hydrologycal models. Positive values of KGE indicate good model performance, while negative KGE values indicate bad model performance (Knoben, 2019; Gupta et al., 2009). The bR^2 values (Krause et al., 2005) are between 0.31 and 0.61 when the intercept is zero and gradients between 0.94 and 1.15. Further on, the performance of ADModel is discussed in Section 5.4 in a wider context, providing a comparison with other models.

5.3 Wider correlations of SRP and OP dynamics to controlling factors, using ADModel-P

In order to understand the underlying phenomena behind these results, correlate it to the modelled transformation rate constants and their controlling factors, and understand in which situations the river is acting as a source or sink Fig. 6 is offered. There are 3 different series of concentration data provided in the same graph: (1) the total value of sources influencing the concentration at M4 (i.e. inputs for M4 which comprise pollution sources, tributaries and the concentration at the upstream end of the stretch, labelled M1); (2) the measurements of concentration at M4 and (3) the simulated concentration at M4.

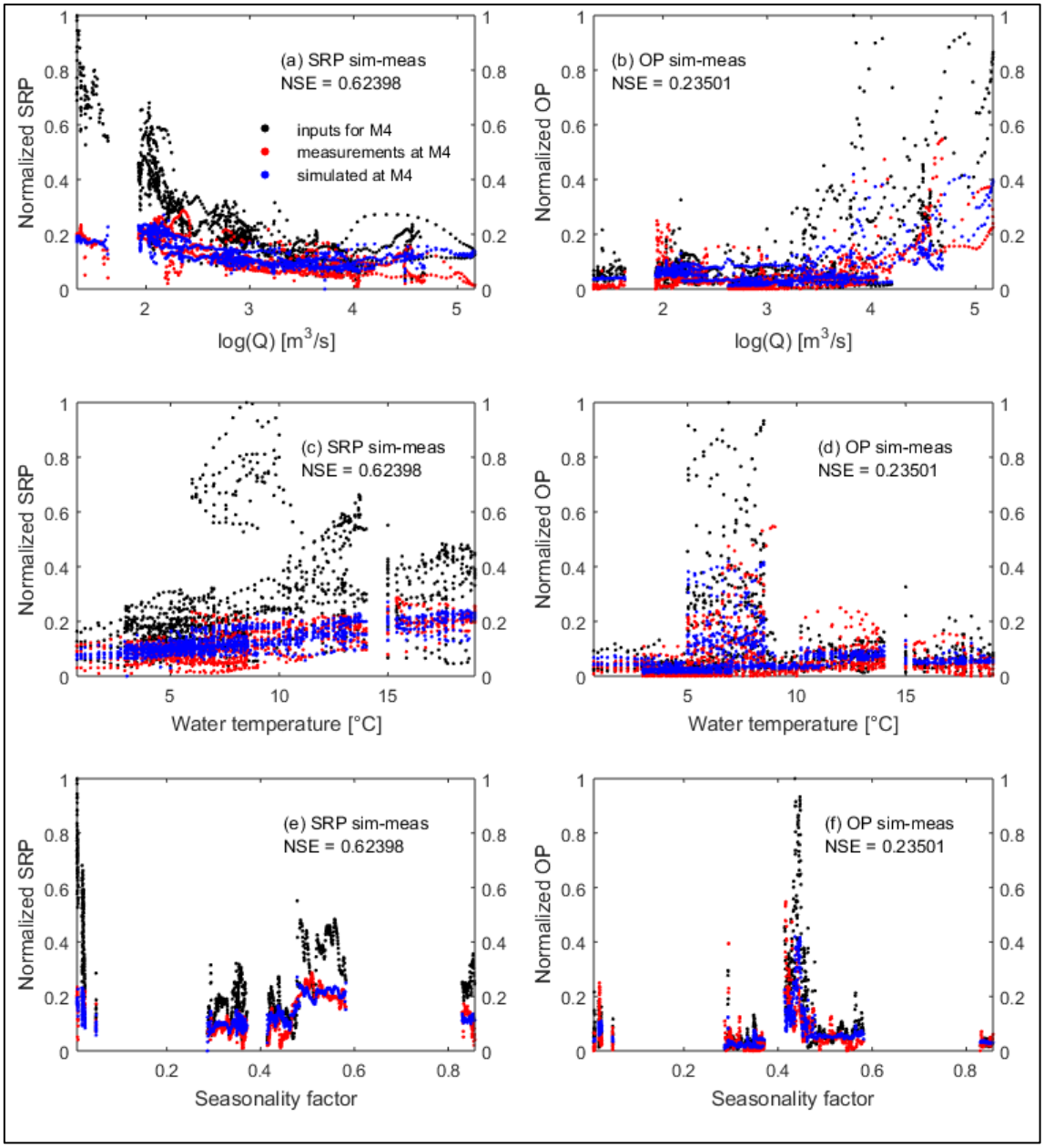

Fig. 6 Normalized values of SRP and OP concentrations (observed, calculated sources and simulated) against water flow (subplots a and b), water temperature (subplots c and d) and seasonality factor (subplots e and f) during the 8 development and calibration campaigns. Normalized values obtained by dividing the actual value of the variable in the dynamic series to the maximum value of all three series.

With respect to water flow (Fig. 6a-b) it is observed that relationships between inputs and outputs are similar below 6 m^3/s (i.e. log(Q) of 1.79 m^3/s) and above 105 m^3/s (i.e. log(Q) of 4.65 m^3/s), where consumption along the stretch occurs for both SRP and OP. At low flows for OP this is attributed to sedimentation, although there is a tendency to overestimate OP concentrations. The sinks of SRP seem to be prominent along the stretch on the entire flow range, except between 22 m^3/s and 55 m^3/s (i.e. log(Q) of 3.09 to 4.01 m^3/s), where there are alternating periods of net sources and sinks (Fig. 6a). For mid-range flows between 6 m^3/s and 105 m^3/s the flow range where the model simulates SRP and OP observations most closely, for OP, there are alternating periods of net sources and sinks. At flows above 105 m^3/s both SRP and OP concentrations are generally overestimated. The implication could be: (1) errors in representation of dilution processes at high flows; (2) additional sinks along the stretch at high flows which are unaccounted for; (3) sinks included in ADModel-P are sufficient but are underestimated at high flows. Refinements increasing the rates of existing sinks may be incorporated if supported by field evidence of other affected in-river conditions (e.g. biotic indicators), but the additional complexity may lead to a less reliable and over parameterised model overall, despite the improved performance.

With respect to water temperature, sinks of SRP are prevalent throughout apart from some occasions above 16 ^oC (Fig. 6c), which may be due to desorption (Fig C.3b). OP sinks and sources alternate along the stretch on the entire temperature range, except between 5 ^oC to 10 ^oC where additional sinks are evident. In this interval, ADModel-P gives better OP predictions compared to temperatures above 12 ^oC when overestimation occurs in multiple occasions.

5.4 With respect to seasonality, there is evidence of SRP sinks at almost all times, except the S range 0.45 to 0.50 (corresponding to mid spring) where there is evidence of SRP sources (Fig. 6e). ADModel-P gives fair predictions, except at S values around 0.45, 0.50 and 0.84 (corresponding to mid-end spring) where SRP is often overestimated, despite the large simulated uptake values. There is no clear evidence

that additional OP sinks or sources are dominant at certain times (Fig. 6f), with the exception of the S range 0.45 to 0.60, where in-stream sinks of OP are evident. Overestimations of OP occur between spring and mid-summer (S above approximatively 0.49), while underestimations occur at the beginning of winter (S around 0.02). It is suspected that accuracy at different seasons may be improved by an improved biotic processes representation (taking into account additional controlling parameters, such as solar radiation or algae), since there is an overestimation of both SRP and OP in spring when biological processes are most significant. Putting findings in the context of other river phosphorus models

ADModel-P represents a phenomena based simulation of phosphorus dynamics in rivers. It differs from other widely available models in that it uses information on river flow, water temperature and seasonality to generate empirical relations to summarise the variation in process rates. Constants (M and R values) are estimated and applied to these functions to generate rate constants (k) values. The rate constants, coupled with zero or first order dependency on the source P pool, define variation in fluxes of phosphorus. In contrast deterministic models such as INCA-P (Jackson-Blake et al., 2016), SWAT (Neitsch et al., 2011), CE-QUAL-W2 (Cole and Wells 2006) and EFDC (Wu and Xu 2011) directly use theoretical relationships along a spectrum of complexity in hydrobiochemical dynamics (for example isotherm kinetics, particulate settling, biotic uptake related to primary productivity) and require a number of additional measurements or assumptions to define these fluxes.

The modelling in the present study demonstrates that if Q, T and S are known then considerable model skill (NSE=0.24-0.62), can be achieved in simulating sub-daily dynamics of OP and SRP in the River Swale system. Evidence from Wellen et al. (2015) suggests that despite a relatively small number of parameters for optimisation (8 empirical coefficients) this compares favourably to other studies at sub-daily resolution. Sub-daily studies are scarce (approximately 2% of studies). Of the studies reviewed

by Wellen et al. (2015) few appear to address identification of in-channel processes reflecting a trend towards whole-basin large-scale system assessment, as identified in Section 1 above.

It is instructive to compare ADModel-P process representation and performance with the Simply-P model (Jackson-Blake et al., 2017) which represents a simplification of INCA-P, having an order of magnitude fewer calibration parameters and achieved without a substantial sacrificing model performance. River particulate phosphorus in Simply P is entirely controlled by particulate behaviour (sedimentation and resuspension). Additionally for dissolved P, although substantial retention has been identified from controlled channel experiments (House et al., 1995), the Simply-P model omits biotic uptake and net adsorption, treating it as a conservative substance within the channel. Jackson-Blake et al. (2017) evaluated the model comparison in a small Scottish rural catchment otherwise similar to the Swale. Short residence time gives limited opportunity for riverine processes to become a significant part of catchment mass-balance. In identifying the importance of net sedimentation and the lack of influence of biotic uptake, the present study corroborates Jackson-Blake et al. (2017), although contrastingly identifies importance of desorption and conversion of inorganic to organic forms to be important. Performance statistics for the two models are broadly similar.

6 Conclusions

ADModel-P is a powerful simulation tool capable to make detailed dynamic predictions, with reasonable accuracy for the case of River Swale. The complexity of phenomena involving P compounds during their transport along the river has been treated with special care during our demarche of finding the optimum representation of transformations included in ADModel-P. Five transformations have been considered (mineralization, sedimentation, resuspension, uptake and adsorption - desorption) and thereby estimated using empirical coefficients catering for a wide range of conditions with respect to water flow, water temperatures and seasonality. The values identified for the coefficients and consequently for the process rates reveal that interaction with sediments and transformation of inorganic P to organic P species are the dominant processes, while the uptake has the lowest influence on inorganic P variability. Simulation results are in agreement with results based on experimental data showing

interactions between water and sediments to be highly significant. Overall, sinks of phosphorus appear to be more important than sources during most of the events studied. Results suggest adsorption-desorption processes are likely to predominate. The rates of interaction with the sediments are highly influenced by the water flow (via the sedimentation and resuspension rates) by the water temperature (via adsorption-desorption rate), and by seasonality (via resuspension rate). The conversion of inorganic to organic forms of P, as well as the mineralization of OP to SRP are influenced by water temperature. The biological uptake of SRP is influenced by the water flow and seasonality.

Model skill has been discussed in the context of the transformation rate coefficients and their main controlling factors. Visual correlations have been offered as support for discussions. Such information can be of additional use as support for other projects related to the identification and formulation of transformation models for different case studies. Work to further improve performance of ADModel-P, may include the estimation of uptake using chlorophyll measurements, or adding new pollutant species for which field data is available (e.g. silica).

Models such as ADModel-P are needed to support water quality management in all rivers. These include those less polluted river networks such as the Ouse of which the Swale is a part, which has been evaluated as oligotrophic/mesotrophic by Hutchins et al. (2010), but with risk of degenerating to a mesotrophic/eutrophic system by 2080. The wider implications from this point of view are the options to adapt ADModel-P to other monitored river stretches over different time-scales which may have levels of accrual or depletion of legacy phosphorus contrasting to those in the Swale in the 1990s. Studies using ADModel to identify change in process rate parameters through a set of sequential applications at intervals before and after undergoing mandatory upgrades in wastewater treatment would improve mechanistic understanding of how river systems respond to interventions and the extent to which legacy effects weaken the expected benefits. The model structure is based on general principles of flow routing pollutant transport and phosphorus transformations and whilst site-specific calibration is necessary it is transferable to any other situation. The approach described here, whereby process rates are estimated

based on readily-available hydro-climatic and seasonal information, can also be used as a means to constrain analogous parameters used in other models.

7 Acknowledgements

This research did not receive any specific grant from funding agencies in the public, commercial, or not-for-profit sectors. We thank Mike Bowes for his knowledge of nutrient dynamics in the Swale River basin. The Environment Agency and Yorkshire Water provided data for model testing.

8 References

1. Alam, M.J., Dutta, D., 2016. A Sub-Catchment Based Approach for Modelling Nutrient Dynamics and Transport at a River Basin Scale, Water Resour. Manag. 30, 5455–5478, DOI 10.1007/s11269-016-1500-x
2. Angert, A., Weiner, T., Mazeh, S., Tamburini, F., Frossard, E., Bernasconi, S.M., Sternberg, M., 2011. Seasonal variability of soil phosphate stable oxygen isotopes in rainfall manipulation experiments, Geochim. Cosmochim. Ac. 75, 4216–4227, DOI:10.1016/j.gca.2011.05.002
3. Ani, E.C., Hutchins, M.G., Kraslawski, A., Agachi, P.Ş., 2011. Mathematical model to identify nitrogen variability in large rivers, River Res. Appl. 27, 1216-1236, DOI 10.1002/rra.1418
4. Ani, E.C., Hutchins M.G., Kraslawski A., Agachi P.Ş., 2010. Assessment of pollutant transport and river water quality using mathematical models, Rev. Roum. Chim. 55, 4, 285-291, WOS:000280213700009
5. Ani, E.C., Avramenko, Y., Kraslawski, A., Agachi, P.Ş., 2009. Selection of models for pollutants transport in river reaches using case based reasoning, Compu.-Aided Chem. En. 27, 537-542, DOI:10.1016/S1570-7946(09)70310-4
6. Boorman, D.B., 2003a. LOIS in-stream water quality modelling. Part 1. Catchments and methods, Sci. Total Environ. 314-316, 379-395.
7. Boorman, D.B., 2003b. LOIS in-stream water quality modelling. Part 2. Results and scenarios, Sci. Total Environ. 314-316, 397-409.

8. Bowes, M.J., Smith, J.T., Jarvie, H.P., Neal, C., 2008. Modelling of phosphorus inputs to rivers from diffuse and point sources, The Sci. Total Environ. 395, 125–138.

9. Bowes, M.J., House, W.A., Hodgkinson R.A., Leach, D.V., 2005. Phosphorus–discharge hysteresis during storm events along a river catchment: the River Swale, UK. Water Res. 39, 751–762.

10. Bowes, M.J., House, W.A., Hodgkinson, R.A., 2003. Phosphorus dynamics along a river continuum, Sci. Total Environ. 313, 199–212.

11. Bowes, M.J., House, W.A., 2001. Phosphorus and dissolved silicon dynamics in the River Swale catchment, UK: a mass-balance approach, Hydrol. Process. 15, 261–280.

12. Bowie, G.L., Mills, W.B., Porcella, D.B., Campbell, C.L., Pagenkopf, J.R., Rupp, G.L., Johnson, K.M., Chan, P.W.H., Gherini, S.A., Chamberlin, C.E., 1985. Rates, constants, and kinetics formulations, Surface Water Quality Modeling. Environmental Research Laboratory, Office of Research and Development, US EPA, EPA/600/3-85/040, 1-472.

13. Caissie, D., Breau, C., Hayward, J., Cameron, P., 2013. Water temperature characteristics of the Miramichi and Restigouche Rivers. Canadian Science Advisory Secretariat, Research Document 2012/165.

14. Charlton, M.B., Bowes, M.J., Hutchins, M.G., Orr, H.G., Soley, R., Davison, P., 2018. Mapping eutrophication risk from climate change: Future phosphorus concentrations in English rivers, Sci. Total Environ. 613–614, 1510–1526.

15. Chau, K.W., 2005. Water Quality Models: Mathematical Framework, in Lehr, J. (Ed.), Water Encyclopedia. Water Quality and Resource Development, John Wiley & Sons, Inc., Hoboken, New Jersey.

16. Colborne, S.F., Maguirea, T.J., Mayer, B., Nightingale, M., Enns, G.E., Fisk, A.T., Drouillarda, K.G., Mohamed, M.N., Weisener, C.G., Wellen, C., Mundle, S.O.C., 2019. Water and sediment as sources of phosphate in aquatic ecosystems: The Detroit River and its role in the Laurentian Great Lakes, Sci. Total Environ. 647, 1594–1603.

17. Cole, T.M., and S. A. Wells, 2006. "CE-QUAL-W2: A two-dimensional, laterally averaged, Hydrodynamic and Water Quality Model, Version 3.5," Instruction Report EL-06-1, US Army Engineering and Research Development Center, Vicksburg, MS, https://pdxscholar.library.pdx.edu/cgi/viewcontent.cgi?article=1129&context=cengin_fac (accessed June 14, 2021).

18. Cooper, R.J., Rawlins, B.G., Krueger, T., Lézé, B., Hiscock, K.M., Pedentchouk, N., 2015. Contrasting controls on the phosphorus concentration of suspended particulate matter under baseflow and storm event conditions in agricultural headwater streams, Sci. Total Environ. 533, 49–59.

19. Dou, M., Cao, Y., Mi, Q., Li, G., Wang, Y., 2018. Multi-phase transformation model of water quality in the sluice-controlled river reaches of Shayinghe River in China, Environ. Sci. Pollut. R. 25, 6633–6647, https://doi.org/10.1007/s11356-017-0991-1

20. Enea, A., Hapciuc, O.E., Iosub, M., Minea, I., Romanescu, G., 2017. Water Quality Assessment in Three Mountainous Watersheds from Eastern Romania (Suceava, Ozana and Tazlau Rivers), Environ. Eng. Manag .J. 16, 3, 605-614.

21. Environment Agency, 2018. The state of the environment: water quality. https://www.gov.uk/government/publications/state-of-the-environment (accessed June 14, 2021)

22. Environment Agency, 2012. WFD River and Lake Classification Data for P. http://www.environment-agency.gov.uk/research/library/data/97343.aspx (accessed September 21, 2020)

23. EEA, 2019. Waterbase, available online at https://www.eea.europa.eu/data-and-maps/indicators/nutrients-in-freshwater/nutrients-in-freshwater-assessment-published-9 (accessed June 14, 2021)

24. Fox, G.A., Purvis, R.A., Penn, C.J., 2016. Streambanks: A net source of sediment and phosphorus to streams and rivers, J. Environ. Manage. 181, 602-614.

25. Gao, L., Li, D., 2014. A review of hydrological/water-quality models, Front. Agric. Sci. Eng. 1(4), 267–276.

26. Gupta, H.V., Kling, H., Yilmaz, K.K. and Martinez, G.F., 2009. Decomposition of the mean squared error and NSE performance criteria: Implications for improving hydrological modelling, J. Hydrol. 377(1-2), 80–91. doi:10.1016/j.jhydrol.2009.08.003

27. Gupta, H.V., Sorooshian, S., Yapo, P.O., 1999. Status of automatic calibration for hydrologic models: Comparison with multilevel expert calibration, J. Hydrologic Eng. 4(2): 135-143.

28. Han, M., Wang, Y., Zhan, Y., Lin, J., Bai, X., Zhang, Z., 2022. Efficiency and mechanism for the control of phosphorus release from sediment by the combined use of hydrous ferric oxide, calcite and zeolite as a geo-engineering tool, Chemical Engineering Journal 428, 131360, doi:10.1016/j.cej.2021.131360

29. Harrison, S., McAree, C., Mulville, W., Sullivan, T., 2019a. The problem of agricultural 'diffuse' pollution: Getting to the point, Sci. Total Environ. 677, 700–717.

30. Harrison, J.A., Beusen, A.H.W., Fink, G., Tang, T., Strokal, M., Bouwman, A.F., Metson, G.S., Vilmin, L., 2019b. Modeling phosphorus in rivers at the global scale: recent successes, remaining challenges, and near-term opportunities, Curr. Opin. Env. Sust. 36, 68–77, https://doi.org/10.1016/j.cosust.2018.10.010

31. House, W.A., 2003. Geochemical cycling of phosphorus in rivers, Appl. Geochem. 18, 739–748.

32. House, W.A., Warwick, M.S., 1999. Interactions of phosphorus with sediments in the River Swale, Yorkshire, UK, Hydrol. Process. 13, 1103-1115.

33. House, W.A., Warwick, M.S., 1998a. Intensive measurements of nutrient dynamics in the River Swale, Sci. Total Environ. 210/211, 111-137.

34. House, W.A., Warwick, M.S., 1998b. A mass-balance approach to quantify the importance of in-stream processes during nutrient transport in a large river Catchment, Sci. Total Environ. 210/211, 111-137.

633 35. House, W.A., Jickells, T.D., Edwards, A.C., Praska, K.E., Denison, F.H., 1998. Reactions of
634 phosphorus with sediments in fresh and marine waters, Soil Use Manage. 14, 139-146.
635 36. House, W.A., Denison, F.H., Armitage, P.D., 1995. Comparison of the uptake of inorganic
636 phosphorus to a suspended and stream bed-sediment, Water Res. 29, 3, 767-779.
637 37. [dataset] Hutchins, M. G., Timis, E. C., 2020. Field data for the development of ADModel,
638 HydroShare, https://doi.org/10.4211/hs.858aaf445ca645f5948a7bd73c16cdd6
639 38. Hutchins, M.G., Williams, R.J., Prudhomme, C., Bowes, M.J., Brown, H., Waylett, A.J.,
640 Loewenthal, M., 2016. Projections of future deteriorations in UK river quality are hampered by
641 climatic uncertainty under extreme conditions, Hydrolog. Sci. J. 61, 16, 2818-2833,
642 http://dx.doi.org/10.1080/02626667.2016.1177186
643 39. Hutchins, M.G., Johnson, A.C., Deflandre-Vlandas, A., Comber, S., Posen, P., Boorman, D., 2010.
644 Which offers more scope to suppress river phytoplankton blooms: Reducing nutrient pollution or
645 riparian shading? Sci. Total Environ. 408, 5065–5077, DOI:10.1016/j.scitotenv.2010.07.033
646 40. Iordache, Ș., Dunea, D., 2013. Multivariate Analysis Applied to Physicochemical Parameters of
647 Treated Wastewater Effluents Discharged in Teleajen River, Rev. Roum. Chim. 58, 7-8, 717-723.
648 41. Jackson-Blake, L. A., Sample, J. E., Wade, A. J., Helliwell, R. C., Skeffington, R. A., 2017. Are
649 our dynamic water quality models too complex? A comparison of a new parsimonious phosphorus
650 model, SimplyP, and INCA-P, Water Resour. Res. 53, 7, 5382-5399,
651 https://doi.org/10.1002/2016WR020132
652 42. Jackson-Blake, L.A., Wade, A.J., Futter, M.N., Butterfield, D., Couture, R.-M., Cox, B.A.,
653 Crossman, J., Ekholm, P., Halliday, S.J., Jin, L., Lawrence, D.S.L., Lepistö, A., Lin, Y., Rankinen,
654 K., Whitehead, P.G., 2016. The INtegrated CAtchment model of phosphorus dynamics (INCA-P):
655 Description and demonstration of new model structure and equations, Environ. Modell. Softw. 83:
656 356-386. DOI:10.1016/j.envsoft.2016.05.022
657 43. Jarvie, H.P., Smith, D.R., Norton, L.R., Edwards, F.K., Bowes, M.J., King, S.K., Scarlett, P.,
658 Davies, S., Dils, R.M., Bachiller-Jareno, N., 2018. Phosphorus and nitrogen limitation and

impairment of headwater streams relative to rivers in Great Britain: A national perspective on eutrophication, Sci. Total Environ. 621, 849–862.

44. Jarvie, H.P., Jurgens, M.D., Williams, R.J., Neal, C., Davies, J.J.L., Barrett, C., White, J., 2005. Role of river bed sediments as sources and sinks of phosphorus across two major eutrophic UK river basins: the Hampshire Avon and Herefordshire Wye, J. Hydrol. 304, 51–74.

45. Jarvie, H.P., Whitton, B.A., Neal, C., 1998. Nitrogen and phosphorus in east coast British rivers: Speciation, sources and biological significance, Sci. Total Environ. 210/211, 79.

46. Ji, Z.G., 2017. Water Quality and Eutrophication, Chapter 5 in Hydrodynamics and Water Quality: Modeling Rivers, Lakes, and Estuaries, 2nd ed. John Wiley & Sons, Inc., Hoboken, NJ (USA).

47. Keraga, A.S., Kiflie, Z., Engida, A.N., 2019. Evaluation of SWAT performance in modeling nutrients of Awash River basin, Ethiopia, Model. Earth Syst. Environ. 5, 275–289, https://doi.org/10.1007/s40808-018-0533-y

48. Kim, K., Kalita, P., Bowes, M.J., Eheart, J.W., 2006. Modeling of river dynamics of phosphorus under unsteady flow conditions, Water Resour. Res. 42, 7, W07413, DOI:10.1029/2005WR004210

49. Knoben, W.J.M., Freer, J.E., Woods, R.A., 2019. Technical note: Inherent benchmark or not? Comparing Nash-Sutcliffe and Kling-Gupta efficiency scores, Hydrol. Earth Syst. Sci. 23, 4323–4331. https://doi.org/10.5194/hess-23-4323-2019

50. Koraqi, H., Luzha, I., Tërmkolli, F., 2016. An Assessment of the Water Quality and Ecological Status of Sitnica River, Kosovo, Studia U Babes-Bol. Che. LXI, 4, 267 – 276.

51. Krause, P., Boyle, D.P., and Base, F., 2005. Comparison of different efficiency criteria for hydrological model assessment, Adv. Geosci. 5, 89-97.

52. [dataset] Leach, D.; Neal, M.; Bachiller-Jareno, N.; Tindall, I.; Moore, R., 2013. Major ion and nutrient data from rivers [LOIS]. NERC Environmental Information Data Centre. (Dataset). Available online at https://catalogue.ceh.ac.uk/documents/4482fa14-aee2-4c7f-9c62-

684 a08dc9704051 (accessed October 30, 2020), https://doi.org/10.5285/4482fa14-aee2-4c7f-9c62-
685 a08dc9704051
686 53. Liberoff, A.L., Flahertya, S., Hualdeb, P., García Asoreya, M.I., Fogel, M.L., Pascual, M.A., 2019.
687 Assessing land use and land cover influence on surface water quality using a parametric weighted
688 distance function, Limnologica 74, 28–37.
689 54. Lindenschmidt, K.E., Fleischbein, K., Baborowski, M., 2007. Structural uncertainty in a river
690 water quality modelling system, Ecol. Model. 204, 289–300.
691 55. Loucks, D.P., van Beek, E, 2017. Water Resources Systems Planning and Management. An
692 Introduction to Methods, Models and Applications, Deltares, UNESCO-IHE, Springer, Chapter
693 10 (Water Quality Modeling and Prediction), Chapter 11 (River Basin Modelling), pp. 417-516.
694 56. Lupi, L., Bertrand, L., Monferrán, M.V., Amé, M.V., Diaz, M.P., 2019. Multilevel and structural
695 equation modeling approach to identify spatiotemporal patterns and source characterization of
696 metals and metalloids in surface water and sediment of the Ctalamochita River in Pampa region,
697 Argentina, J. Hydrol. 572, 403–413.
698 57. Mateus, M., da Silva Vieira, R., Almeida, C., Silva, M., Reis, F., 2018. ScoRE - A Simple
699 Approach to Select a Water Quality Model, Water 10, 1811, DOI:10.3390/w10121811Mbabazi,
700 J., Inoue, T., Yokota, K., Saga, M., 2019. Phosphorus bioavailability in rivers flowing through
701 contrasting land uses, Journal of Environmental Chemical Engineering 7, 102960,
702 doi:10.1016/j.jece.2019.102960
703 58. Moriasi, D.N., Arnold, J.G., Van Liew, M.W., Bingner, R.L., Harmel, R.D., Veith, T.L., 2007.
704 Model evaluation guidelines for systematic quantification of accuracy in watershed simulations,
705 Transactions of the ASABE 50(3), 885-900.
706 59. Nash, J.E, Sutcliffe, J.V., 1970. River flow forecasting through conceptual models: Part I A
707 discussion of principles, J. Hydrol. 27(3): 282–291, http://dx.doi.org/10.1016/0022-
708 1694(70)90255-6

709 60. [dataset] National River Flow Archive (UK), Live data: NRFA archived flows and near real-time
710 flows from the Environment Agency's Hydrology API. Available online at
711 https://nrfa.ceh.ac.uk/data/search (accessed on October, 30, 2020).
712 61. Neal, C., Jarvie, H.P., Withers, P.J.A., Whitton, B.A., Neal, M., 2010. The strategic significance
713 of wastewater sources to pollutant phosphorus levels in English rivers and to environmental
714 management for rural, agricultural and urban catchments, Sci. Total Environ. 408, 1485–1500.
715 62. Nguyen, T.T., Keupers, I., Willems, P., 2018. Conceptual river water quality model with flexible
716 model structure, Environ. Modell. Softw. 104, 102-117,
717 https://doi.org/10.1016/j.envsoft.2018.03.014
718 63. Neitsch, S.L., Arnold, J.G., Kiniry, J.R., Williams, J.R., 2011. Soil and Water Assessment Tool
719 Theoretical Documentation, Version 2009, Texas Water Resources Institute Technical Report No.
720 406. Texas A&M University System: College Station, TX,
721 https://swat.tamu.edu/media/99192/swat2009-theory.pdf (accessed June 14, 2021)
722 64. Ockenden, M.C., Deasya, C.E., Benskin C.McW.H., Beven, K.J., Burke, S., Collins, A.L., Evans,
723 R., Falloon, P.D., Forber, K.J., Hiscock, K.M., Hollaway, M.J., Kahana, R., Macleodi, C.J.A.,
724 Reaney, S.M., Snell, M.A., Villamizar, M.L., Wearing, C., Withers, P.J.A., Zhou, J.G., Haygarth,
725 P.M., 2016. Changing climate and nutrient transfers: Evidence from high temporal resolution
726 concentration-flow dynamics in headwater catchments, Sci. Total Environ. 548–549, 325–339.
727 65. Owens, P.N., Walling, D.E., 2003. Temporal changes in the metal and phosphorus content of
728 suspended sediment transported by Yorkshire rivers, U.K. over the last 100 years, as recorded by
729 overbank floodplain deposits, Hydrobiologia 494, 185–191.
730 66. Pujol, Ll., Sanchez-Cabeza, J.A., 2000. Use of tritium to predict soluble pollutants transport in
731 Ebro River waters (Spain), Environ. Pollut. 108, 257-269.
732 67. Ramos, T.B., Gonçalves, M.C., Branco, M.A., Brito, D., Rodrigues, S., Sánchez-Pérez, J.M.,
733 Sauvage, S., Prazeres, A., Martins, J.C., Fernandes, M.L., Pires, F.P., 2015. Sediment and nutrient

734 dynamics during storm events in the Enxoé temporary river, southern Portugal, Catena 127, 177–
735 190.
736 68. Records, R.M., Wohl. E., Arabi, M., 2016. Phosphorus in the river corridor, Earth-Sci. Rev. 158,
737 65–88.
738 69. Riley, W.D., Potter, E.C.E., Biggs, J., Collins, A.L., Jarvie, H.P., Jones, J.I., Kelly-Quinn, M.,
739 Ormerod, S.J., Sear, D.A., Wilby, R.L., Broadmeadow, S., Brown, C.D., Chanin, P., Copp, G.H.,
740 Cowx, I.G., Grogan, A., Hornby, D.D., Huggett, D., Kelly, M.G., Naura, M., Newman, J.R.,
741 Siriwardena, G.M., 2018. Small Water Bodies in Great Britain and Ireland: Ecosystem function,
742 human-generated degradation, and options for restorative action, Sci. Total Environ. 645, 1598–
743 1616.
744 70. Robson, B.J., 2014. State of the art in modelling of phosphorus in aquatic systems: Review,
745 criticisms and commentary, Environ. Modell. Softw. 61, 339–359.
746 doi:10.1016/j.envsoft.2014.01.012
747 71. Romanescu, G., Hapciuc, O.E., Sandu, I., Minea, I., Dascalita, D., Iosub, M., 2016. Quality
748 Indicators for Suceava River, Rev. Chim - Bucharest 67, 2, 245-249.
749 72. Smith, B.P.G., Naden, P.S., Leeks, G.J.L., Wass, P.D., 2003. The influence of storm events on fine
750 sediment transport, erosion and deposition within a reach of the River Swale, Yorkshire, UK, Sci.
751 Total Environ. 314 –316, 451–474.
752 73. Srinivas, R., Singh, A.P., 2018. An integrated fuzzy-based advanced eutrophication simulation
753 model to develop the best management scenarios for a river basin, Environ. Sci. Pollut. R. 25,
754 9012–9039.
755 74. Tang, T., Strokal, M., Van Vliet, M.T.H., Seuntjens, P., Burek, P., Kroeze, C., Langan, S., Wada,
756 Y., 2019. Bridging global, basin and local-scale water quality modeling towards enhancing water
757 quality management worldwide, Curr. Opin. Env. Sust. 36, 39–48,
758 DOI:10.1016/j.cosust.2018.10.004

759 75. [software] Timis, E.C., 2021. ADModel for phosphorus compounds (ADModel-P), HydroShare,
760 https://doi.org/10.4211/hs.6b2cde0ea82b439d83cf96f5b61aa1f6
761 76. Tsakiris, G., Alexakis, D., 2012. Water quality models: An overview, Eur. Water 37, 3-46.
762 77. Tuo, Y., Chiogna, G., Disse, M., 2015. A Multi-Criteria Model Selection Protocol for Practical
763 Applications to Nutrient Transport at the Catchment Scale, Water 7, 2851-2880,
764 DOI:10.3390/w7062851
765 78. Tye, A.M., Rawlins, B.G., Rushton, J.C., Price, R., 2016. Understanding the controls on sediment-
766 P interactions and dynamics along a non-tidal river system in a rural urban catchment: The River
767 Nene, Appl. Geochem. 66, 219-233.
768 79. Wade, A.J., Whitehead, P.G., Butterfield, D., 2002. The Integrated Catchments model of
769 Phosphorus dynamics (INCA-P), a new approach for multiple source assessment in heterogeneous
770 river systems: model structure and equations, Hydrol. Earth Syst. Sc. 6(3), 583–606.
771 80. Wang, Q., Li, S., Jia, P., Qi, C., Ding, F., 2013. A Review of Surface Water Quality Models, The
772 Scientific World Jo. Article ID 231768, 1-7. http://dx.doi.org/10.1155/2013/231768
773 81. Wellen, C., Kamran-Disfani, A.-R., Arhonditsis, G.B., 2015. Evaluation of the Current State of
774 Distributed Watershed Nutrient Water Quality Modeling, Environ. Sci. Tech. 49, 3278-3290,
775 DOI:10.1021/es5049557
776 82. Wijesiri, B., Liu, A., Deilami, K., He, B., Hong, N., Yang, B., Zhao, X., Ayoko, G., Goonetilleke,
777 A., 2019. Nutrients and metals interactions between water and sediment phases: An urban river
778 case study, Environ. Pollut. 251, 354-362.
779 83. Withers, P.J.A., Jarvie, H.P., 2008. Delivery and cycling of phosphorus in rivers: A review, Sci.
780 Total Environ. 400, 1–3, 379-395.
781 84. Wu, G., Xu, Z., 2011. Prediction of algal blooming using EFDC model: Case study in the Daoxiang
782 Lake, Ecol. Model. 222 (6), 1245-1252, DOI: 10.1016/j.ecolmodel.2010.12.021
783 85. Yuan, S., Tang, H., Xiao, Y., Xia, Y., Melching, C., Li, Z., 2019. Phosphorus contamination of
784 the surface sediment at a river confluence, J. Hydrol. 573, 568–580.

785 86. Zelenakova, M., Purcz, P., Pintilii, R.D., Blistan, P., Hlustik, P., Oravcova A., Hashim, M.A.,
786 2018. Spatio-temporal Variations in Water Quality Parameter Trends in River Waters, Rev. Chim
787 - Bucharest, 69, 10, 2940-2947.
788 87. Zinabu, E., Kelderman, P., van der Kwast, J., Irvine, K., 2018. Evaluating the effect of diffuse and
789 point source nutrient transfers on water quality in the Kombolcha River Basin, an industrializing
790 Ethiopian catchment, Land Degrad. Dev. 29, 3366–3378, DOI: 10.1002/ldr.3096
791 88. Zhang, W., Swaney, D.P., Hong, B., Howarth, R.W., 2017. Anthropogenic Phosphorus Inputs to
792 a River Basin and Their Impacts on Phosphorus Fluxes along its Upstream-Downstream
793 Continuum, J. Geophys, Res.-Biogeo. 122, 3273-3287, DOI:10.1002/2017jg004004
794

Appendix A

Table A. 1 Phosphorus main forms/ compounds in the river.

P form/ components	Short explanation
SRP **Soluble Reactive Phosphorus**	Measurable component. Routinely termed also: Phosphates; Orthophosphates; Ortho-phosphorus; Bioavailable Phosphorus, Dissolved Inorganic Phosphorus (DIP), Dissolved Reactive Phosphorus (DRP), Inorganic Phosphorus (IP), Molybdate Reactive Phosphorus (MRP), Filterable Reactive Phosphorus (FRP). The labile phosphorus component in water. The SRP fraction is biologically available. Largely equivalent to Total Reactive Phosphorus (TRP), the most relevant component when assessing the eutrophication risk.
SUP **Soluble Unreactive Phosphorus**	Sometimes referred to as Dissolved Hydrolysable Phosphorus (DHP). The non-labile component of the TDP. It represents a mixture of polymeric inorganic phosphorus, colloidal material and organo-phosphorus compounds: Soluble Organic Phosphorus (SOP) and Soluble Complex Phosphorus (SCP). Calculated (not measured) as TDP – SRP. SOP and SCP compose the Dissolved Organic Phosphorus (DOP) denomination used often as equivalent to SUP.
TDP **Total Dissolved Phosphorus**	Measurable component. Composed of the labile (SRP) and no-labile (SUP) components in water, presented as soluble inorganic and soluble organic P. Only a part of the dissolved organic P is considered immediately available.
TP **Total Phosphorus**	Measurable component. Composed of SUP (DHP), SRP and PP. In particular cases, where it is assumed that most of the dissolved TP is unreactive, TP consists of SUP and PP.
PP **Particulate Phosphorus**	PP (PPS or POP) is the more available component of the suspended sediments that breaks down with acid oxidation to generate SRP. It contains organic phosphorus. Calculated (not measured) as PP = TP –TDP or PP = TP – SUP (in particular cases, where it is assumed that most of the dissolved TP is unreactive).

Appendix B

Table B. 1 Goodness of fit associated to non-conservative ADModel-P runs in different options of splitting the data for preliminary calibration and evaluation (NSE – Nash Sutcliffe model efficiency criteria)

Run number	Campaigns used for evaluation	NS during calibration runs		NS during evaluation runs	
		SRP	OP	SRP	OP
1.	1, 10	0.45	0.21	-0.36	-0.02
2.	2, 9	0.44	0.20	-0.24	0.34
3.	2, 8	0.49	0.25	0.56	-0.18
4.	3, 6	0.41	0.09	0.16	-0.02
5.	3, 10	0.41	0.21	0.69	-0.32
6.	4, 7	0.52	0.23	-0.29	-0.41
7.	5, 10	0.50	0.21	-0.26	-0.21
8.	6, 7	0.48	0.06	0.14	-0.01
9.	6, 8	0.46	-0.12	-0.11	-0.18
10.	7, 10	0.48	0.22	0.26	-0.03
11.	8, 10	0.47	0.24	0.75	0.18
12.	9, 10	0.45	0.13	0.48	-0.02

802 **Table B. 2 Criteria employed for the assessment of ADModel-P performance**

Model evaluation criteria	Equation	References
Nash Sutcliffe efficiency (NSE)	$NSE = 1 - \frac{\sum_{i=1}^{n}(O_i - P_i)^2}{\sum_{i=1}^{n}(O_i - \bar{O})^2}$ n is the total number of samples, i the individual samples, O the observations, P the predictions, and $\bar{O}$ the mean of observations.	Nash and Sutcliffe (1970) Moriasi et al. (2017) Gupta et al. (2009)
Percent bias (PBIAS)	$PBIAS = \frac{\sum_{i=1}^{n}(O_i - P_i)}{\sum_{i=1}^{n} O_i} 100$	Moriasi et al. (2007) Gupta et al. (1999)
Root mean square error ratio to observations standard deviation (RSR)	$RSR = \frac{\sqrt{\sum_{i=1}^{n}(O_i - P_i)^2}}{\sqrt{\sum_{i=1}^{n}(O_i - \bar{O})^2}}$	Moriasi et al. (2007)
Kling-Gupta Efficiency (KGE)	$KGE = 1 - \sqrt{(r-1)^2 + \left(\frac{\sigma_P}{\sigma_O} - 1\right)^2 + \left(\frac{\bar{P}}{\bar{O}} - 1\right)^2}$ $r = \frac{Cov_{PO}}{\sigma_P \, \sigma_O}$ r is the linear correlation coefficient between predictions and observations, Cov_{PO} the covariance between the predictions and observed values, σ_P and σ_O the standard deviations of predictions and observations, and $\bar{P}$ the mean of predictions.	Knoben et al. (2019) Gupta et al. (2009)
Modified coefficient of determination (bR^2)	$bR^2 = \begin{cases} \lvert b \rvert R^2 \; for \; b \leq 1 \\ \lvert b \rvert^{-1} R^2 \; for \; b > 1 \end{cases}$ $R^2 = \left(\frac{\sqrt{\sum_{i=1}^{n}(O_i - \bar{O})(P_i - \bar{P})}}{\sqrt{\sum_{i=1}^{n}(O_i - \bar{O})^2} \sqrt{\sum_{i=1}^{n}(P_i - \bar{P})^2}} \right)^2$ b is the slope of the regression line between predictions and observations when the intercept is zero or very close to zero, R^2 the coefficient of determination defined as the square of the coefficient of correlation according to Bravais-Pearson.	Krause et al. (2005)

803

Appendix C

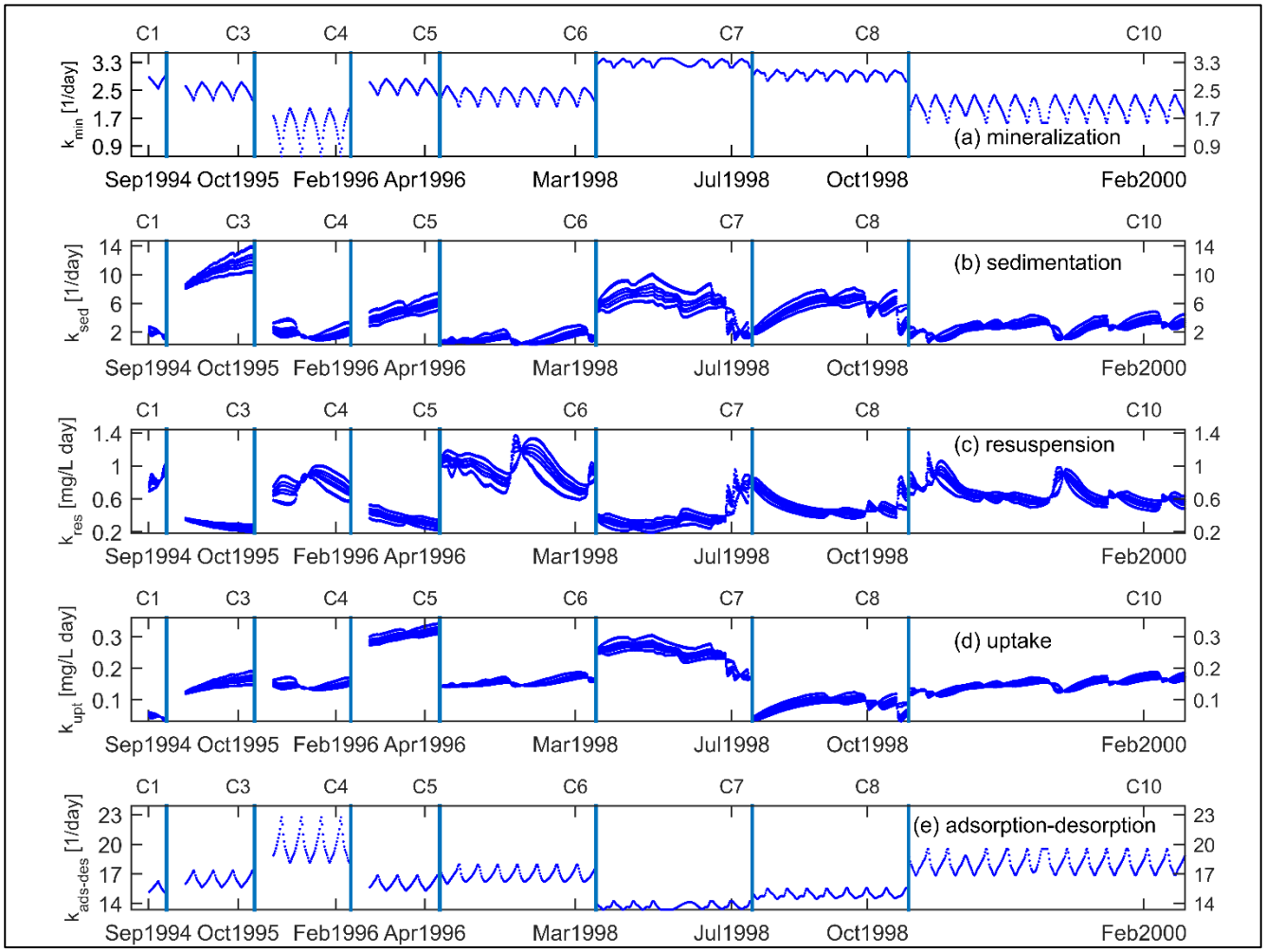

Fig. C.1 Dynamic evolution of transformations rate constants used by ADModel-P during calibration (subplot a - mineralization, subplot b - sedimentation, subplot c - resuspension, subplot d - uptake, subplot e – adsorption-desorption). The time x-axes are not continuous. Data from the individual campaigns C1 to C10 carried out during the specified months (Table 1) has been concatenated during simulations. The vertical lines mark the boundaries between C1 to C10.

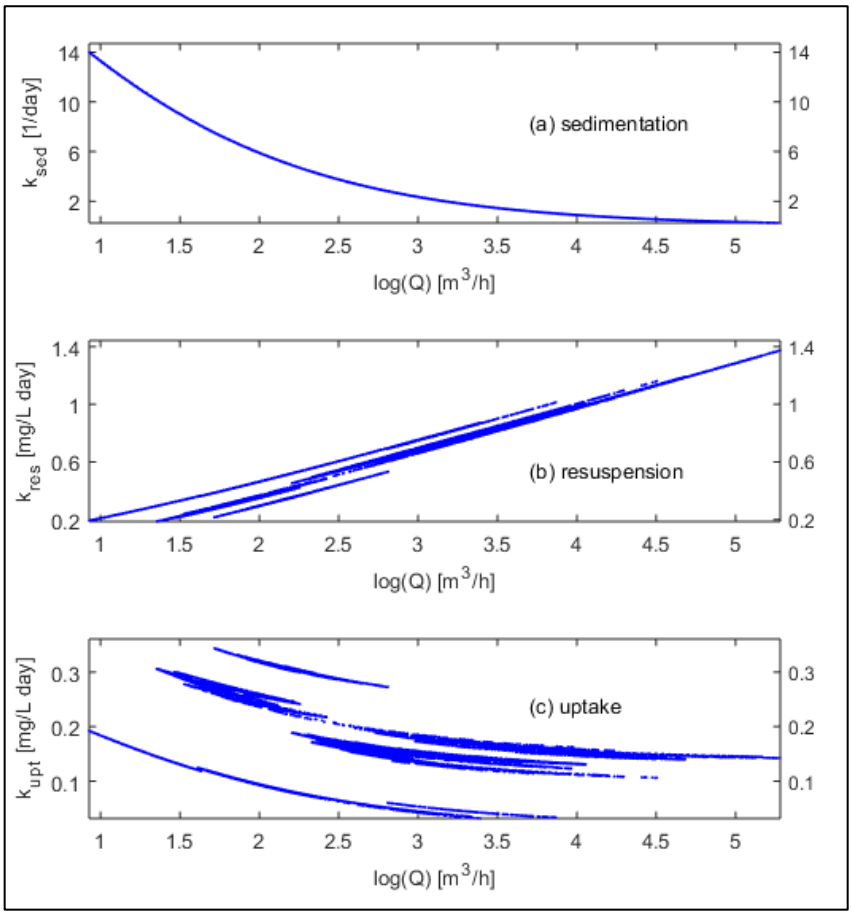

Fig. C.2 The dependence on water flow of the transformation rate constants used by ADModel-P during calibration (subplot a - sedimentation, subplot b - resuspension, subplot c - uptake).

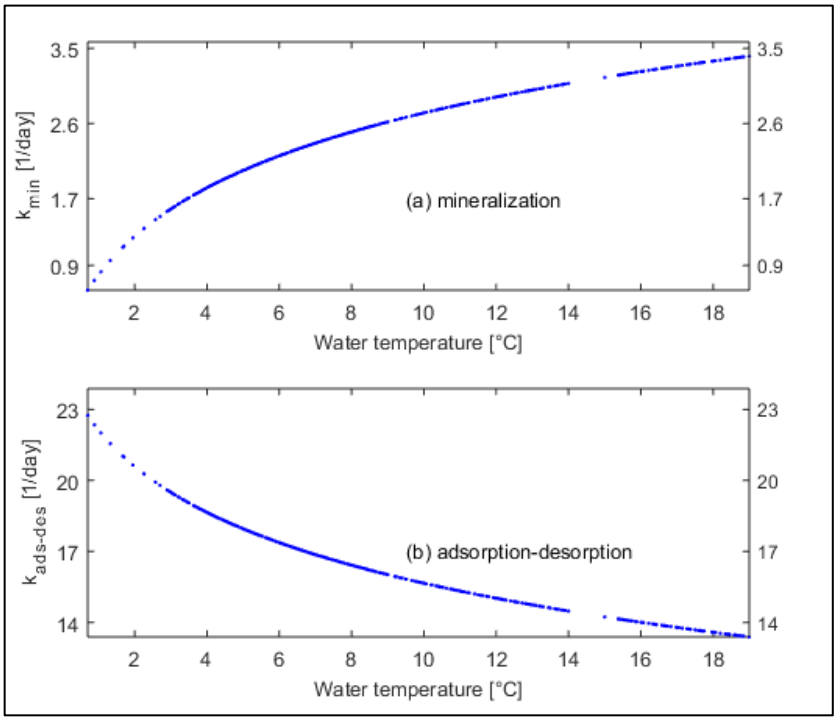

Fig. C.3 The dependence on water temperature of the transformation rate constants used by ADModel-P during calibration (subplot a - mineralization, subplot b – adsorption-desorption).

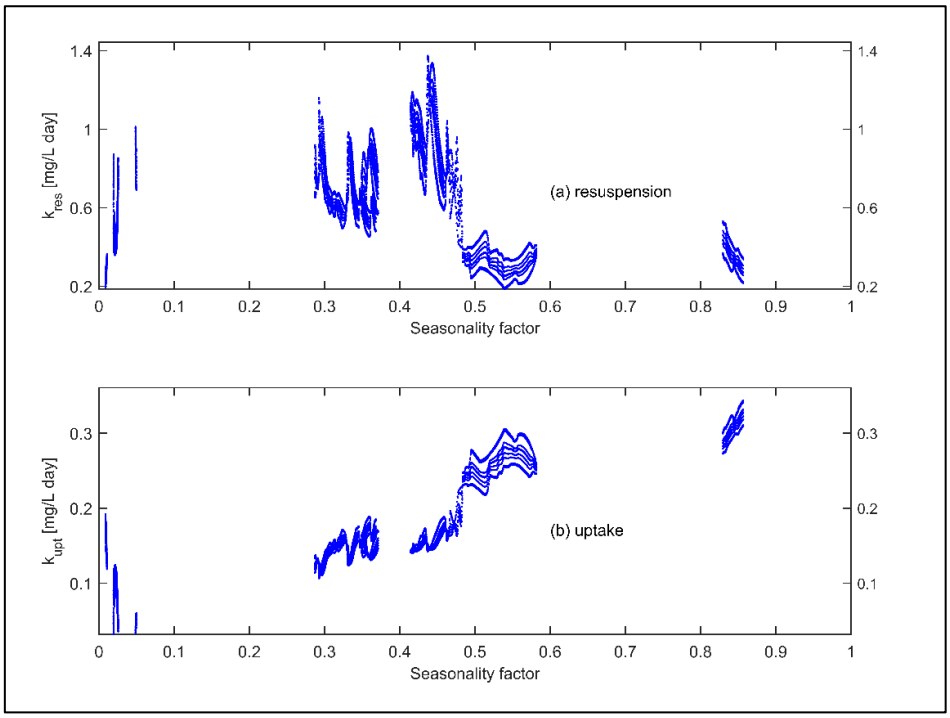

Fig. C.4 The dependence on the seasonality factor of the transformation rate constants used by ADModel-P during calibration (subplot a - resuspension, subplot b - uptake).

Appendix D

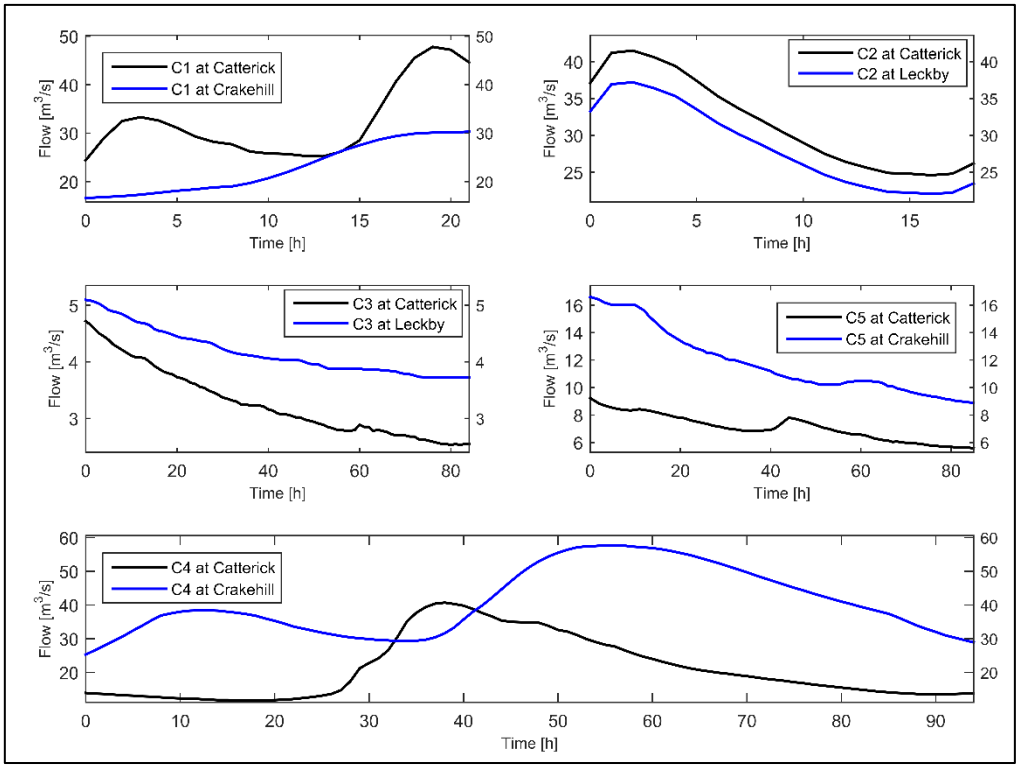

Fig. D. 1 The dynamics of water flow at the upper and lower end of the stretch during the monitoring campaigns C1 to C5.

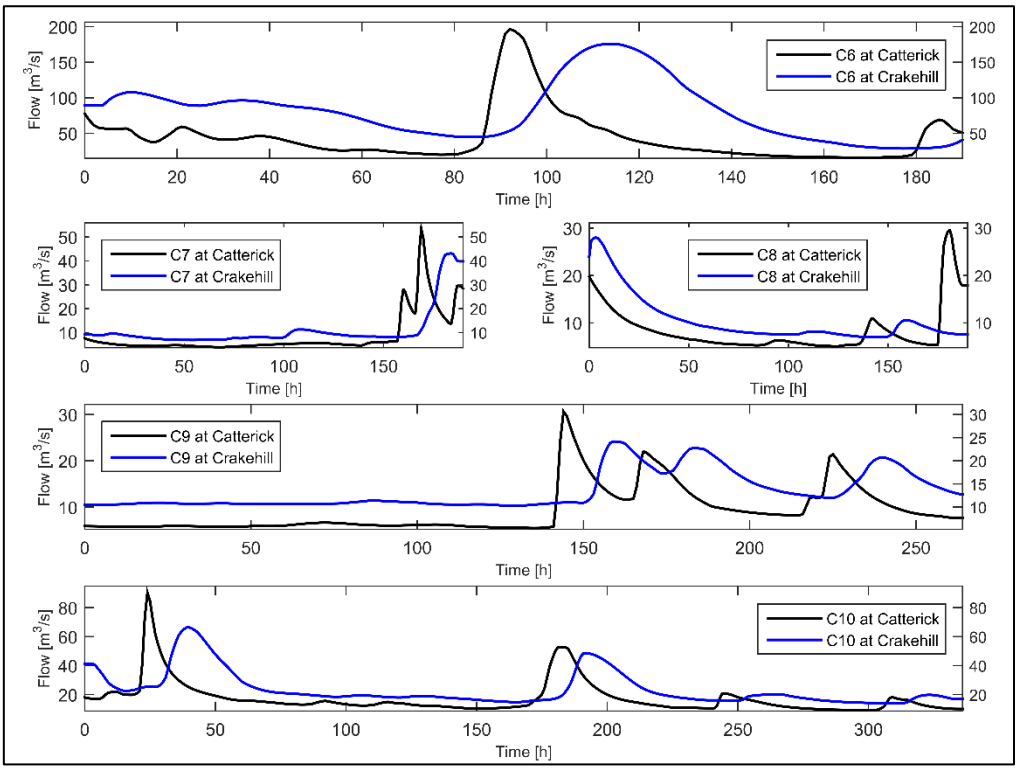

Fig. D. 2 The dynamics of water flow at the upper and lower end of the stretch during the monitoring campaigns C6 to C10.

Appendix E

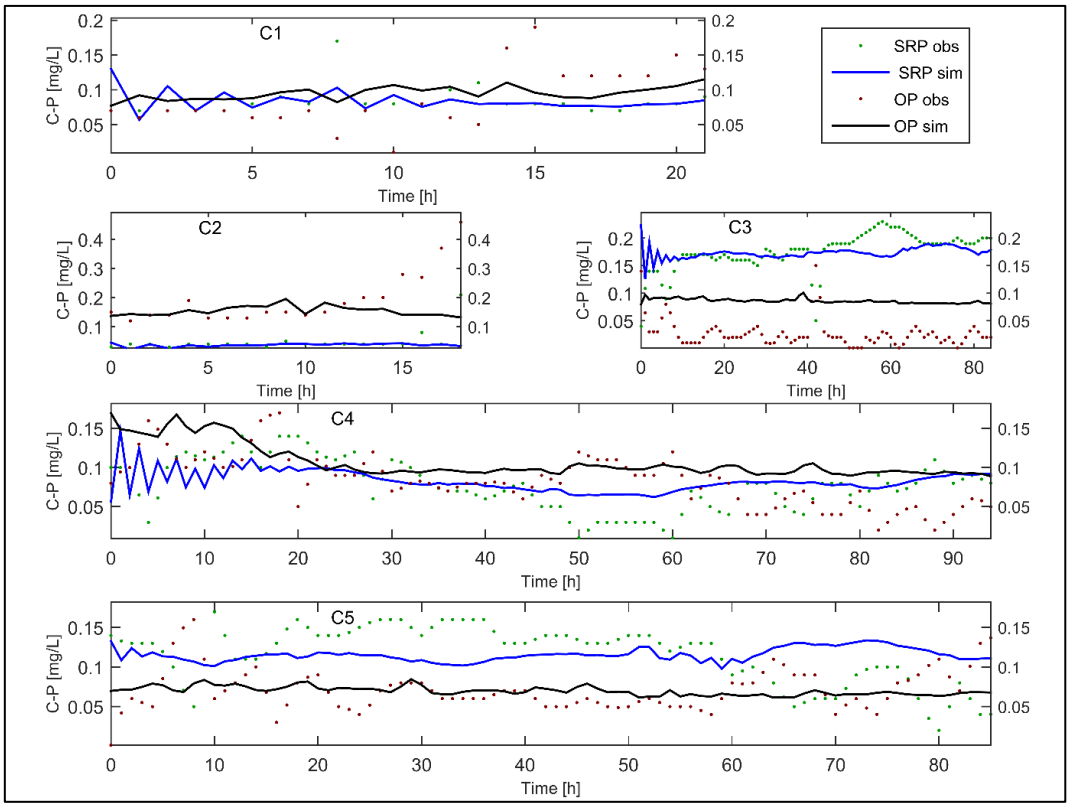

Fig. E. 1 Dynamic profiles of the observed (obs) and simulated (sim) concentration (C-P [mg/L]) of SRP and OP during campaigns C1 to C5 presented at hourly resolution at the downstream end of the river stretch.

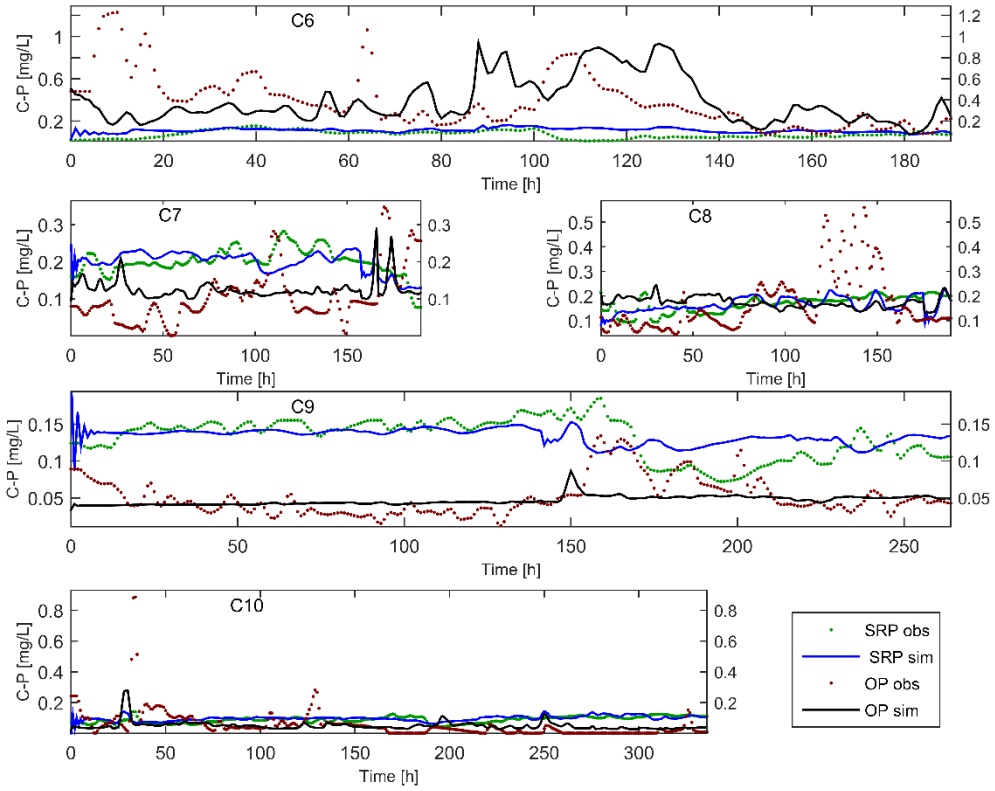

Fig. E. 2 Dynamic profiles of the observed (obs) and simulated (sim) concentration (C-P [mg/L]) of SRP and OP during campaigns C6 to C10 presented at hourly resolution at the downstream end of the river stretch.